Cancer Management and Research

Dovepress

open access to scientific and medical research

Open Access Full Text Article

ORIGINAL RESEARCH

Psoralen Suppresses Cisplatin-Mediated Resistance and Induces Apoptosis of Gastric Adenocarcinoma by Disruption of the miR196a-HOXB7-HER2 Axis

This article was published in the following Dove Press journal:
Cancer Management and Research

Lei Jin[1,2,*]
Xue-Mei Ma[1,2,*]
Ting-Ting Wang[1,2]
Yao Yang[1,2]
Nan Zhang[2,3]
Na Zeng[2,4]
Zhi-Gang Bai[1,2]
Jie Yin[1,2]
Jun Zhang[1,2]
Guo-Qian Ding[1,2]
Zhong-Tao Zhang[1,2]

[1]Department of General Surgery, Beijing Friendship Hospital, Capital Medical University, Beijing, People's Republic of China; [2]National Clinical Research Center for Digestive Diseases, Beijing, People's Republic of China; [3]Department of Radiology, Beijing Friendship Hospital, Capital Medical University, Beijing, People's Republic of China; [4]Clinical Epidemiology and EBM Center, Beijing Friendship Hospital, Capital Medical University, Beijing, People's Republic of China

*These authors contributed equally to this work

Correspondence: Guo-Qian Ding; Zhong-Tao Zhang
Email dingguoqian@gmail.com; zhangzhongtao@ccmu.edu.cn

Purpose: The present study aimed to investigate the impact of psoralen on miR-196a-5p expression and function, and to reveal the mechanism underlying miR-196a-5p-mediated inhibition and the reversal of cisplatin (DDP) resistance.

Methods: Serum samples were collected from 50 patients with gastric cancer (GC), and the association between miR-196a-5p expression and the response to chemotherapy was assessed. A DDP-resistant GC cell line was also established to determine the effects of miR-196a-5p and psoralen on DDP resistance. MGC803 cells were transfected with miR-196a-5p mimic and inhibitor vectors for the overexpression and downregulation of miR-196a-5p, respectively.

Results: Clinical data analysis showed that the lower expression levels of miR-196a-5p were significantly associated with chemoresistance in patients with GC. Upregulation of miR-196a-5p significantly enhanced the anti-proliferative effect, apoptosis and sensitivity to DDP by regulating the protein expression levels of HOXB7, HER2, Bcl-2 and G_1/S-specific cyclin-D1 (CCND1). Furthermore, psoralen reversed miR-196a-5p-induced DDP resistance and reduced the expression levels of HOXB7, HER2, Bcl-2 and CCND1.

Conclusion: miR-196a-5p may be a novel biomarker of chemotherapeutic success in patients with GC and may also influence the sensitivity of GC cells to DDP. Moreover, psoralen can increase chemotherapeutic sensitivity by upregulating miR-196a-5p and then downregulating HOXB7-HER2 signaling axis.

Keywords: miR-196a-5p, psoralen, chemoresistance, cisplatin, gastric cancer, HOXB7

Introduction

Gastric cancer (GC) is ranked as the fourth most malignant tumor, as well as the second leading cause of tumor-related death worldwide.[1] There were about 691 000 cases of gastric adenocarcinoma worldwide in 2012.[2] An estimated 720 000 patients died from gastric cancer in that year.[3] Surgery is the first choice of treatment for patients with early-stage GC, but since recurrence is frequent, a combination of surgery and chemotherapy is frequently used.[4] Compared with surgery alone, combined therapy improved disease-free survival rate and reduced the risk of recurrence and metastasis in a number of clinical trials.[5]

Among different chemotherapeutic agents, cisplatin (DDP) is a first-line choice for patients with progressive GC. DDP can activate several pathways which promote apoptosis, thus exerts an antitumor effect.[6] Due to the high incidence of drug-resistance, metastasis and recurrence, the long-term survival of patients with GC is unsatisfactory.[7] DDP resistance is inevitable in most patients, and results in

submit your manuscript | www.dovepress.com
DovePress
http://doi.org/10.2147/CMAR.S248094

treatment failure. Furthermore, long-term use and repeated administration of DDP are associated with severe side effects.[8] Hence, the discovery of novel biomarkers and targets for chemotherapy-resistant GC, and elucidating the underlying molecular mechanisms of chemoresistance, are critical for improving prognosis and treatment efficacy.

Despite demonstrated alterations and mutations in a number of GC-associated genes, the underlying molecular mechanisms for chemotherapeutic resistance and GC development have yet to be clarified. The upregulation of HER2 has been observed in various drug-resistant cancer types, though the mechanisms involved are poorly understood.[9] Therefore, identification of the mechanisms of resistance to HER2 targeting, and proposing a feasible strategy for their circumvention in GC, would be of significant clinical value. Previous studies have revealed that HOXB7, an estrogen receptor (ER) cofactor for HER2 activation, promotes endocrine resistance.[10] Moreover, the overexpression of HOXB7 induces cellular proliferation, which is associated with poor patient outcome in GC.[11] Therefore, the HOXB7-HER2 axis may serve a vital role in the molecular mechanisms underlying the chemotherapeutic resistance of GC.

MicroRNAs (miRNAs) are a recently discovered class of 19–25 nucleotide small non-coding RNAs that can negatively regulate target gene expression by inhibiting expression or promoting the degradation of mRNA.[12] Aberrant miRNA expression has been reported in various types of human cancer, and their participation in cancer angiogenesis, immune evasion, tumor growth and invasion indicate that miRNAs serve vital roles in cellular regulation.[13–20] miRNAs have also been associated with drug resistance, and their dysregulation has reportedly been linked to DDP resistance in numerous types of tumor.[21–24] However, the roles of miRNAs in GC etiology and its response to chemotherapy are not fully understood. Illuminating the biological influences of miRNA dysregulation, as well as their target genes, is crucial to the elucidation of their cellular functions. The underlying mechanisms of miRNA dysregulation and antineoplastic drug resistance may be associated with miRNA-mediated regulation of apoptosis and proliferation, which may subsequently block DNA repair and drug targeting.[25]

MicroRNA-196a-5p (miR-196a-5p) is a member of the miR-196 family. miR-196a-5p appears to have originated from the intergenic regions of homeobox gene clusters in a number of species, and is a basic early-stage regulator of tail regeneration.[26,27] Downregulated miR-196a-5p expression has been identified in various malignancies, including breast, colorectal and non-small-cell lung cancer; though there are currently few studies of the effect of miR-196a-5p on GC drug resistance.[28,29] As a result, the present study aimed to determine the underlying mechanisms of miR-196a-5p downregulation and the reversal of DDP resistance in MGC803/DDP cells. Previous studies have suggested that a combination of chemotherapy and miRNA regulation may be a promising treatment option for patients with chemo-resistant cancer. Hence, altering the level of miR-196a-5p expression may be a prospective strategy for combatting DDP resistance in human GC.

In addition, the expression levels of specific miRNAs in the serum of patients with tumors can predict treatment sensitivity and prognosis in a number of cancer types.[30–32] Moreover, there is emerging evidence that specific serum miRNAs may aid the early diagnosis and detection of malignancies, as well as survival prognosis for patients following surgery.[33–35] Nevertheless, unique miRNAs that predict the response to GC chemotherapy remain undiscovered. In the present study, the association between clinical outcome and miRNA expression was assessed using serum samples from patients with GC following DDP-based first-line treatment. The serum miRNA signature may have predictive value for the DDP response and provide a useful biomarker for personalized therapy.

Traditional Chinese Medicine has received considerable attention for its potential use against multi-drug resistance (MDR).[36] Natural products play a critical role for the treatment of various types of cancers via different mechanisms.[37–39] Psoralen, the primary active ingredient of *Psoralea Corylifolia*, is used as an anticancer agent, though its mechanism of action remains unclear. Previous studies have indicated that psoralen effectively inhibits the progression of cutaneous T-cell lymphoma, and exerts a certain degree of cytotoxicity towards mucoepidermoid carcinoma cells.[40–42]

Several agents have been investigated for the effective reversal of DDP resistance. However, there are currently no successfully developed drugs in clinical use. In the present study, the reversal effect of psoralen on DDP resistance was investigated in GC cell lines. Specifically, the effect of psoralen on cell cycle progression and proliferation, mediated by miR196a-HOXB7-HER2 pathway, was analyzed in MGC803 and MGC803/DDP cells. Furthermore, DDP/psoralen combination treatment was assessed for its potential synergistic effect on GC cells. Additionally, the clinical significance and biological function of miR-196a-5p was clarified, as well as its effect on DDP resistance in GC.

Materials and Methods

Reagents and Antibodies

Primary antibodies against the following targets were obtained from: HOXB7 (40-2000; Invitrogen; Thermo Fisher Scientific, Inc.), HER2 (22425; Cell Signaling Technology, Inc.), β-actin (SAB5500001; Sigma-Aldrich; Merck KGaA), and cyclin D1 (29225; Cell Signaling Technology, Inc.) and Bcl-2 (15071T; Cell Signaling Technology, Inc.). The secondary antibodies (7074S and 7076S) were also purchased form Cell Signaling Technology, Inc. DDP (purity, >99%; HPLC, 10 mg) and psoralen (purity >99%; HPLC, 10 mg) were acquired from Sigma-Aldrich; Merck KGaA.

Cell Culture

The MGC803 cell line was acquired from the Chinese Academy of Medical Sciences (Beijing, China). To establish a DDP-resistant GC cell line (MGC803/DDP), MGC803 cells were cultured in the presence of 2.5 μg/mL DDP in a continuous stepwise manner, which drug concentrations ranged from low to high, for 10 months, which resulted in a shift towards a proliferative and anti-apoptotic phenotype. The cell line was continuously cultured with 1 μg/mL DDP to maintain resistance. Psoralen-cultured cells were continuously cultured with psoralen for 4 weeks, unless otherwise indicated. The cell lines were authenticated by STR profiling, and the profiles compared with the ATCC, DSMZ or JCRB databases (Cobioer Biosciences Co., Ltd). The cells were cultured in Dulbecco's Modified Eagle Medium (DMEM), supplemented with 10% fetal bovine serum (FBS), 100 IU/mL penicillin and 100 IU/mL streptomycin (all Gibco; Thermo Fisher Scientific, Inc.), in a humidified cell incubator with an atmosphere of 5% CO_2 at 37°C, and the MGC803/DDP cell line was cultured without DDP for a week prior to subsequent experimentation.

Transfection

Expression plasmids for the miR-196a-5p mimic control, miR-196a-5p mimic, miR-196a-5p inhibitor control and miR-196a-5p inhibitor were purchased from Fulengene. For further study, including flow cytometry, reverse transcription-quantitative (RT-q) PCR and Western blotting, cells were seeded into 6-well plates (Corning Inc.) at a concentration of $5x10^5$/well; for MTT assays, the cells were seeded into 96-well plates at $4x10^3$/well. When the cells had reached ~80% confluence, each expression plasmid was mixed with Opti-MEM™ I (Invitrogen; Thermo Fisher Scientific, Inc.) and incubated for 5 min. Next, EndoFectin™-Max transfection reagent (GeneCopoeia, Inc.) was diluted in Opti-MEM™ I and incubated for 5 min. The plasmids were then added to the diluted transfection reagent to form a transfection complex, which was then incubated for 10 min. Finally, the mixtures were added to each well and incubated in a humidified cell incubator with an atmosphere of 5% CO_2 at 37°C for 48–72 h. The cells were then collected, and transfection efficiency was confirmed by RT-qPCR and Western blotting. All experiments were carried out at room temperature.

Patient Enrollment

Serum specimens from 50 patients with GC in Beijing Friendship Hospital, Capital Medical University were collected according to the following criteria: i) Gastric adenocarcinoma was histologically confirmed; ii) patients had received DDP-based chemotherapy as a first-line treatment; iii) patients had received ≥2 cycles of chemotherapy; and iv) chemotherapeutic efficacy was evaluated by unenhanced and enhanced computed tomography (CT) after 2 or 3 cycles. The present study was approved by the Ethics Committee of Beijing Friendship Hospital, Capital Medical University, and was conducted following the principles of the Declaration of Helsinki. All patients gave written informed consent prior to blood sample collection. Pre-chemotherapy serum samples from patients who had received neoadjuvant chemotherapy or palliative treatment were collected between January 2015 and December 2018. The chemotherapeutic response was evaluated by 2 radiologists according to Choi's criteria.[43] Treatment resistance was viewed as existing progressive disease (PD) in <3 treatment cycles, and treatment response was viewed as existing complete response (CR), stable disease (SD) or partial response (PR) lasting for 2 or 3 cycles. Chemotherapy response-sensitive consisted of CR and PR, and chemotherapy response-resistant included SD and PD.

MTT Assay

To verify the chemoresistance of the MGC803/DDP cell line, cells were either cultured under normal conditions, or in the presence of DDP or psoralen as aforementioned. The cells were then seeded into a 96-well plate at a concentration of $4x10^3$/well, and after adherence, were treated with DDP and psoralen (200 μL/well) at the indicated concentrations, either as a single drug or in combination, for 48 h. The negative control cells were treated with the vehicle only. After the cells in 96-well plates were incubated with the MTT reagent (3-(4, 5-dimethylthiazol-2-yl)-2, 5-diphenyltetrazolium bromide) at 37°C for 4 h, the culture medium was removed, and then 200 μL dimethyl sulfoxide (DMSO) was added to

dissolve the formazan. The OD values were recorded at 569 nm using a microplate reader (Bio-Rad Laboratories, Inc.). IC_{10} and IC_{50} values were calculated and cell survival curves were generated using GraphPad Prism 7 (GraphPad Software, Inc.).

Colony Formation Assay

Briefly, 500 cells/well were added to a 6-well plate and cultured for 3 days under drug treatment, and subsequently cultured in complete medium without DDP for 2 weeks. Colonies were fixed with anhydrous methanol and stained with crystal violet (0.1% w/v) dye. Viable colonies that contained ≥50 cells were counted and the mean colony number was calculated. Colony forming efficiency was defined as the percentage of the colony number to the number of plated cells; relative colony forming efficiency was defined as the colony forming efficiency of the treated sample/that of the untreated sample. Cells were plated in triplicate for each condition.

Flow Cytometric Analysis of Apoptosis

Cells were treated with various concentrations of DDP or psoralen (or a combination of both) or the vehicle control for 48 h, and subsequently harvested. The cells were then double-stained with propidium iodide and fluorescein isothiocyanate-Annexin V (BD Biosciences), and subsequently analyzed using a FACSCalibur flow cytometer (BD Biosciences). The levels of apoptosis were determined using FlowJo Software version 10 (FlowJo LLC).

RNA Extraction and RT-qPCR

Total RNA was extracted from the cell lines and patient samples using TRIzol® reagent (Invitrogen; Thermo Fisher Scientific, Inc.). The RNA quality and concentration were determined using a spectrophotometer (Thermo Fisher Scientific, Inc.). The primers for miRNA and mRNA detection were purchased from FulenGene, and the sequences are shown in Table 1. For miRNA analysis, total RNA was reverse transcribed and quantified using the All-in-One™ miRNA RT-qPCR Kit (GeneCopoeia, Inc.). Relative miRNA expression was normalized to that of U6 or let-7g-5p. For mRNA analysis, total RNA was reverse transcribed using the FastQuant RT Kit (Tiangen Biotech Co., Ltd.) and qPCR was conducted using the Power SYBR® Green PCR master mix (Toyobo Life Science). mRNA expression was normalized to that of β-actin or GAPDH. A pre-incubation for 10 min at 95°C was followed by 40 amplification cycles: 10 sec at 95°C, 20 sec at 60°C and 10 sec at 72°C. All reactions were performed using the ABI 7500 real-time fast PCR system (Applied Biosystems).

Table 1 Primers Used for RT-qPCR Analysis

Symbol	Primer	Primer Sequence
miR-196a-5p	Forward	5′-GGGCTAGGTAGTTTCATGTTG-3’
miR-196a-5p	Reverse	5′-AGTGCGTGTCGTGGAGTC-3’
HOXB7	Forward	5′-GGAAAAAGGAGAACAAGACCG-3’
HOXB7	Reverse	5′-CTCCATCCCTCACTCTTCCTC-3’
HER2	Forward	5′-AGATTCCGGGAGTTGGTGTC-3’
HER2	Reverse	5′-GTCATCGTCCTCCAGCAGTG-3’
Bcl-2	Forward	5′-TGTCCCTTTGACCTTGTTTCT-3’
Bcl-2	Reverse	5′-TCATTTGCCATCTGGATTTT-3’
CCND1	Forward	5′-TGTCCTACTACCGCCTCACAC-3’
CCND1	Reverse	5′-TTGGGGTCCATGTTCTGC-3’

Abbreviations: HOXB7, Homeobox B7; HER2, human epidermal growth factor receptor 2; Bcl-2, B-cell lymphoma-2; CCND1, G1/S-specific cyclin-D1.

Western Blotting

Whole protein was extracted from the harvested cells using RIPA lysis buffer, and quantified with a bicinchoninic acid protein assay kit (Beyotime Institute of Biotechnology). The proteins were separated using a 10% SDS-PAGE gel (Invitrogen; Thermo Fisher Scientific, Inc.) and electrotransferred onto PVDF membranes (GE Healthcare Bio-Sciences). The membranes were blocked for 2 h with 5% non-fat dried milk, and incubated with primary antibodies against HOXB7 (1:1000), HER2 (1:1000), β -actin (1:5000), cyclin D1 (1:1000), and Bcl-2 (1:1000) at 4°C overnight. The following day, the membranes were washed and incubated with the corresponding secondary antibodies (1:5000) for 1 h at 37°C. The target proteins were visualized using Novex™ ECL Chemiluminescent Substrate Reagent Kit (Invitrogen; Thermo Fisher Scientific, Inc.) and analyzed using Image Lab™ Software version 3.0 (Bio-Rad Laboratories, Inc.).

Dual-Luciferase Reporter Assay

The HOXB7 3′-UTR (containing the putative miR-196a-5p binding sites) was cloned into the PmiR-RB-Report™ dual-luciferase reporter vector (Guangzhou RiboBio Co. Ltd.). Using the EndoFectin™-Max transfection reagent (GeneCopoeia, Inc.), MGC803 cells were transfected with the following: HOXB7-WT/NC vector, HOXB7-WT vector + miR-196a-5p mimic, HOXB7-MUT/NC vector, or HOXB7-MUT vector + miR-196a-5p mimic. Lipo6000™ transfection reagent (Beyotime Biotechnology, Inc.) was used for cell transfection. Culture medium was replaced 6 h after transfection. The luciferase activity values were

calculated 48–72 h post-transfection. In this assay, firefly luciferase was used as the experimental reporter gene, and *Renilla* luciferase was used as the control reporter gene. Experimental reporter genes were used to test gene expression under experimental conditions, while control reporter genes were used as internal controls to normalize the results of experimental reporter tests.

Bioinformatics Analysis

TargetScan (www.targetscan.org) was used to identify potential downstream target genes, and to predict the conserved putative binding sequence for miR-196a-5p. Additionally, the Kaplan–Meier Plotter (http://kmplot.com) was used to determine the association between the expression levels of miRNA and mRNAs and patient overall survival (OS) over a 10-year period.[44]

Statistical Analysis

The association between miR-196a-5p expression and patient clinicopathological parameters was analyzed using the Mann–Whitney *U*-test. The expression level distribution of mir-196a-5p in different groups is presented as the median and interquartile range [median (Q1 and Q3)]. The Log rank test was used to determine significant differences between groups during Kaplan–Meier analysis. All data are expressed as the mean ± standard deviation, and each experiment was independently repeated ≥3 times. Quantitative data were analyzed and graphically represented using GraphPad Prism 7. For the in vitro experiments, statistical differences were analyzed using the unpaired Student's t-test and one-way ANOVA followed by Tukey's multiple comparisons test. *P<0.05 was considered to indicate a statistically significant difference.

Results

Analysis of Drug-Resistant Cell Lines

To verify the chemoresistance of the MGC803/DDP cell line, MGC803/DDP and MGC803 cells were treated with various concentrations of DDP for 48 h, and cell viability was assessed (Figure 1A). The DDP IC_{50} value for MGC803/DDP cells (~5.99 μg/mL) was 10.2-fold higher than that of the MGC803 cells (~0.59 μg/mL) (Figure 1B). Colony formation (Figure 1C and D) and flow cytometric assays (Figure 1E and F) were also used to compare DDP resistance between the MGC803/DDP and MGC803 cell lines. Furthermore, RT-qPCR revealed that miR-196a-5p expression was reduced ~37.0-fold in MGC803/DDP, compared with MGC803 cells (Figure 2A), which confirmed the association between DDP resistance and miR-196a-5p expression level. These results suggest that miR-196a-5p expression may affect the sensitivity of GC cells to DDP.

Expression Levels and Functions of miR-196a-5p in Human GC Specimens

The clinicopathological characteristics of 50 patients who received neoadjuvant chemotherapy or palliative treatment are displayed in Table 2. The distribution of miR-196a-5p expression in different groups is presented as the median and interquartile range [median (Q1 and Q3)]. Clinical data were collected and treatment efficacy was evaluated by CT after 2 or 3 cycles of chemotherapy. Independent measurements were made by 2 radiologists according to Choi's criteria. A combination of unenhanced and enhanced CT was applied to accurately evaluate the tumor response according to the tumor density measurement. The serum miR-196a-5p expression levels in 25 chemotherapy response-sensitive (CR and PR) and 25 chemotherapy response-resistant (SD and PD) patients were analyzed by RT-qPCR. The results show that miR-196a-5p expression was reduced in the serum of patients with chemotherapy response-resistant GC (Figure 2B). The association between clinical parameters and miR-196a-5p expression was also assessed. The upregulation of miR-196a-5p was significantly associated with smaller tumor size (P=0.0135; Figure 2C) and weakly associated with TNM stage (P=0.0664). However, the miR-196a-5p level was not related to age, sex or lymph metastasis. These results indicate that in patients with GC, miR-196a-5p may serve as a marker for the response to DDP treatment.

To ascertain the potential of miR-196a-5p as a prognostic factor, a large cohort analysis of survival data was performed using the Kaplan–Meier Plotter. Patients with high miR-196a-5p levels (n=107) exhibited longer OS times over a 10-year period, compared with those with low miR-196a-5p levels (n=324, HR=0.73, P=0.063; Figure 2E). This was particularly pronounced in patients of Asian origin (n=87, HR=0.41, P=0.027; Figure 2F). Moreover, the area under the curve (AUC) suggested a certain degree of diagnostic value (0.8552; Figure 2D). These observations indicate that low miR-196a-5p expression is associated with chemoresistance and poor patient survival, implicating miR-196a-5p upregulation as a potential treatment option for patients with DDP-resistant GC.

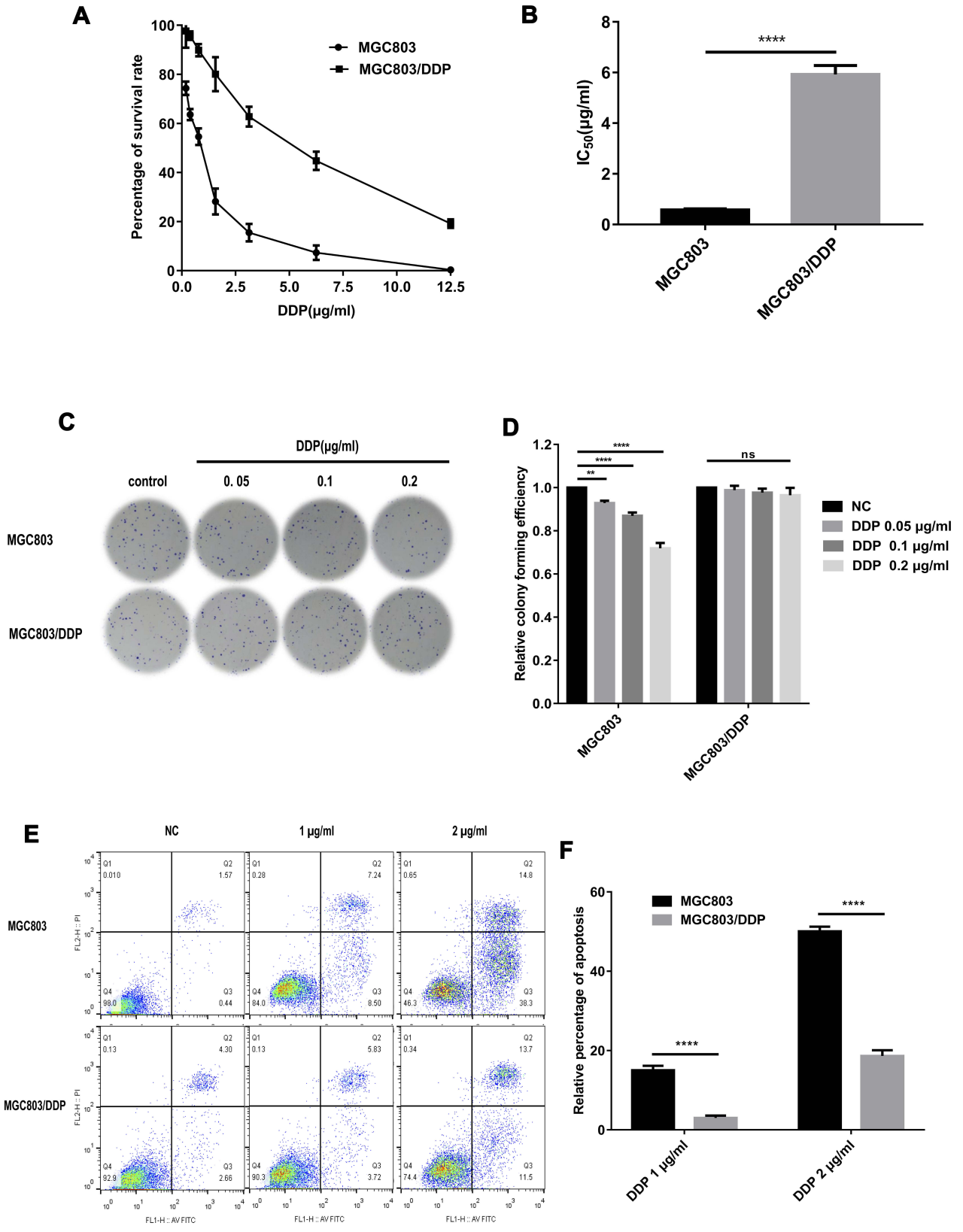

Figure 1 Identification of drug-resistant cell lines. (**A** and **B**) MTT assay was used to examine cell activity (**A**) and the 50% inhibition concentration (IC_{50}) values (**B**) of MGC803/DDP and MGC803 cell lines. (**C** and **D**) DDP resistance (**C**) and cell proliferation ability (**D**) between MGC803/DDP cells and MGC803 cells was evaluated via colony formation assay. (**E** and **F**) DDP resistance (**E**) and cell apoptosis rates (**F**) were examined in MGC803/DDP and MGC803 cells via flow cytometry assay. Each assay was conducted in triplicate. ****P < 0.0001, **P < 0.01 and mean±SD were utilized to show the data.

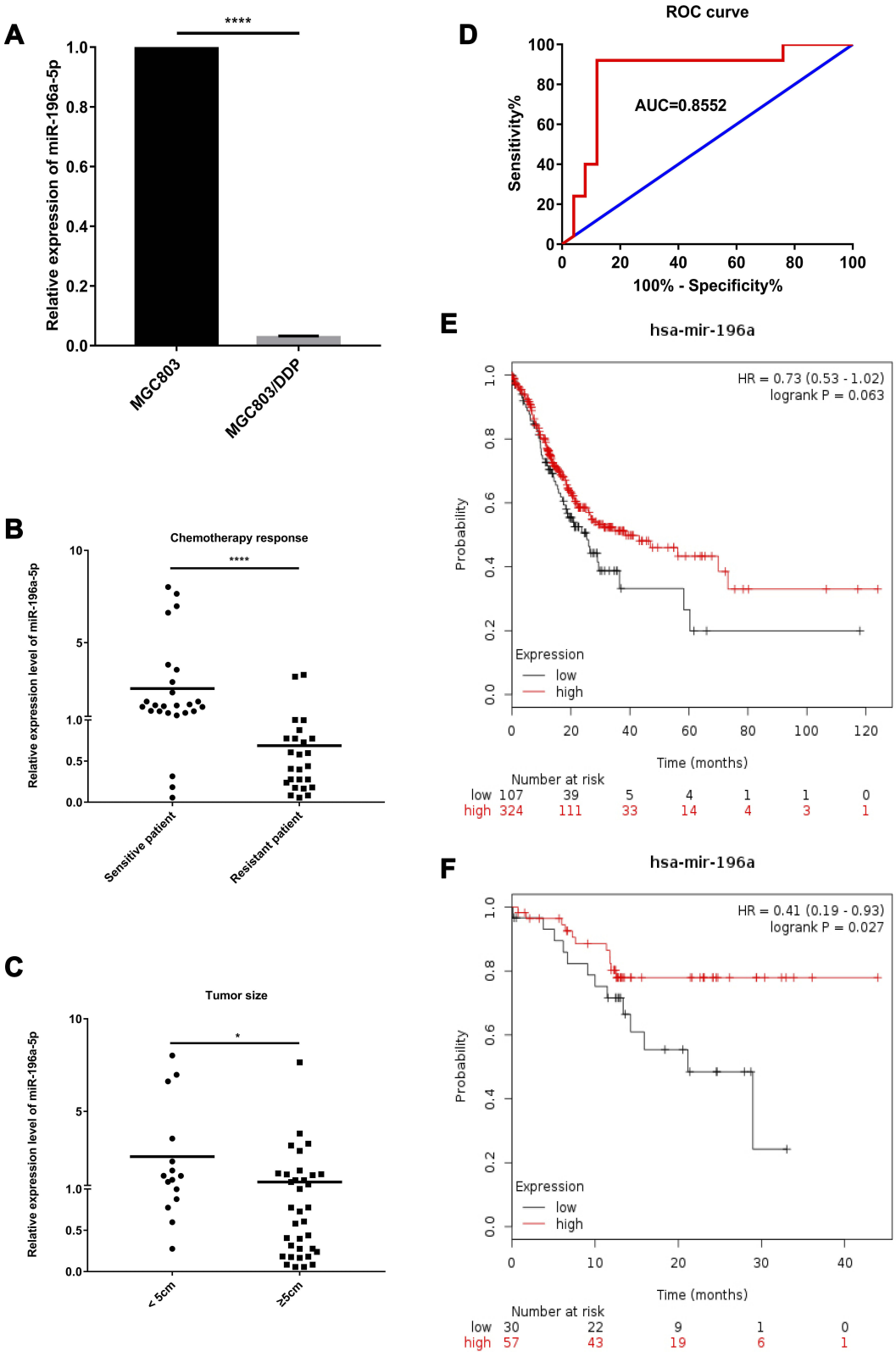

Figure 2 Expression levels and functions of miR-196a-5p in human GC clinical specimens. (**A**) The relative miR-196a-5p level between parental MGC803 cells and DDP-resistant MGC803/DDP cells was analyzed via RT-qPCR. (**B**) The relative miR-196a-5p level between 25 chemotherapy response-sensitive gastric cancer serums and 25 chemotherapy response-resistant gastric cancer serums was measured using RT-qPCR. (**C**) The relevance of miR-196a-5p level with tumor size was analyzed via RT-qPCR. (**D**) ROC curve and AUC value in comparison of the prognostic accuracy for DDP response with the miR-196a-5p expression. (**E**) Kaplan–Meier survival curves suggested that lower miR-196a-5p levels (n=107) were correlated with lower patient survival rates other than higher miR-196a-5p levels (n=324) according to Kaplan–Meier Plotter. (**F**) Kaplan–Meier survival curves suggested that lower miR-196a-5p levels (n=30) were relevant with lower patient survival rates other than higher miR-196a-5p levels (n=57) according to Kaplan–Meier Plotter, especially in Asian patients. Each assay was conducted in triplicate. ****P < 0.0001, *P < 0.05 and mean±SD were utilized to show the data.

Table 2 The Correlation Between miR-196a-5p Expression and Clinical Parameters in GC Patients (n=50)

Clinical Parameters	Cases (n)	Expression Level	P value
Age (years)			0.5247
<60	14	1.2840 (0.8769, 1.6370)	
≥60	36	0.7745 (0.3055, 1.6466)	
Gender			0.1203
Male	40	1.0267 (0.5447, 1.6562)	
Female	10	0.2490 (0.1685, 1.5564)	
Tumor Size (cm)			0.0135*
<5	15	1.5146 (0.9378, 2.9162)	
≥5	35	0.7281 (0.2575, 1.5735)	
Lymph Metastasis			0.2819
Absent	3	2.0518 (1.4144, 3.0137)	
Present	47	0.8263 (0.3055, 1.5635)	
TNM Stage			0.0664
III	6	3.2522 (1.7643, 5.4497)	
IV	44	0.9983 (0.3566, 1.5999)	
Chemotherapy Response			<0.0001*
Sensitive (CR+PR)	25	0.4387 (0.2387, 0.7747)	
Resistant (SD+PD)	25	1.5936 (1.2840, 2.8661)	

Notes: Expression levels are shown with median and quartile spacing. *$p < 0.05$.
Abbreviations: CR, complete response; PR, partial response; SD, stable disease; PD, progressive disease.

Exogenous Overexpression and Downregulation of miR-196a-5p in GC Cell Lines

The aforementioned results suggested that the miR-196a-5p expression level in MGC803/DDP cells was ~37.0-fold lower than that of the MGC803 cell line; thus miR-196a-5p was subsequently overexpressed in MGC803/DDP cells and downregulated in MGC803 cells by transient transfection. The RT-qPCR results confirm that miR-196a-5p level was significantly reduced in MGC803 cell transfected with the inhibitor, compared with that in the control cells (Figure 3A). By contrast, the miR-196a-5p levels in the MGC803/DDP cell line were markedly increased by transfection with an miR-196a-5p mimic, compared with the control cells (Figure 3B), therefore confirming transfection efficiency.

Downregulation of miR-196a-5p Renders MGC803 Cells Resistance to DDP

To demonstrate the association between miR-196a-5p downregulation and DDP resistance in GC cell lines, MGC803 cells were transfected with either an miR-196a-5p inhibitor or the associated negative control. The cells were then treated with a range of DDP concentrations for 48 h, after which viability was assessed (Figure 3C). miR-196a-5p-knockdown in MGC803 cells resulted in an increased survival rate, a higher DDP IC_{50} value and reduced rate of apoptosis, compared with the control cells (Figure 3D). Following treatment with 0.1 μg/mL DDP for 2 weeks, reduced levels of miR-196a-5p were also associated with increased proliferation and colony formation, (Figure 3E and F). In addition, flow cytometric analysis revealed that after treatment with 0.5 μg/mL DDP for 48 h, MGC803 cells transfected with miR-196a-5p inhibitor exhibited decreased apoptotic rate compared with the control cells (Figure 3G and H). Therefore, miR-196a-5p-knockdown MGC803 cells exhibited greater DDP resistance, with a significant decrease in cytotoxicity and apoptosis. The results suggest that downregulation of miR-196a-5p increases DDP resistance in MGC803 cells.

Overexpression of miR-196a-5p Sensitizes MGC803/DDP Cells to DDP

To demonstrate the association between DDP resistance and miR-196a-5p overexpression, MGC803/DDP cells were transfected with either an miR-196a-5p mimic or the corresponding negative control. Cellular activity was detected following treatment with various concentrations of DDP for 48 h (Figure 4A). MGC803/DDP cells transfected with the miR-196a-5p mimic showed a marked decrease in survival rate, a lower DDP IC_{50} value and higher rates of apoptosis, compared with the control cells (Figure 4B). High levels of miR-196a-5p were associated with decreased cell proliferation after 2 weeks of culture with 0.5 μg/mL DDP (Figure 4C and D). Furthermore, MGC803/DDP cells transfected with different levels of miR-196a-5p mimic exhibited increased rates of apoptosis following culture with 2 μg/mL DDP for 48 h, compared with the control cells (Figure 4E and F). Therefore, miR-196a-5p overexpression decreased DDP resistance, with a prominent increase in cytotoxicity and apoptosis. These results demonstrate that miR-196a-5p upregulation decreases DDP resistance in the MGC803/DDP cell line.

HOXB7 Is a Target Gene for miR-196a-5p

miR-196a-5p has been shown to regulate DDP resistance in breast cancer, at least in part by inhibiting HOXB7.[10] To further elucidate the underlying mechanisms of miR-196a-5p-associated GC cell apoptosis under DDP treatment,

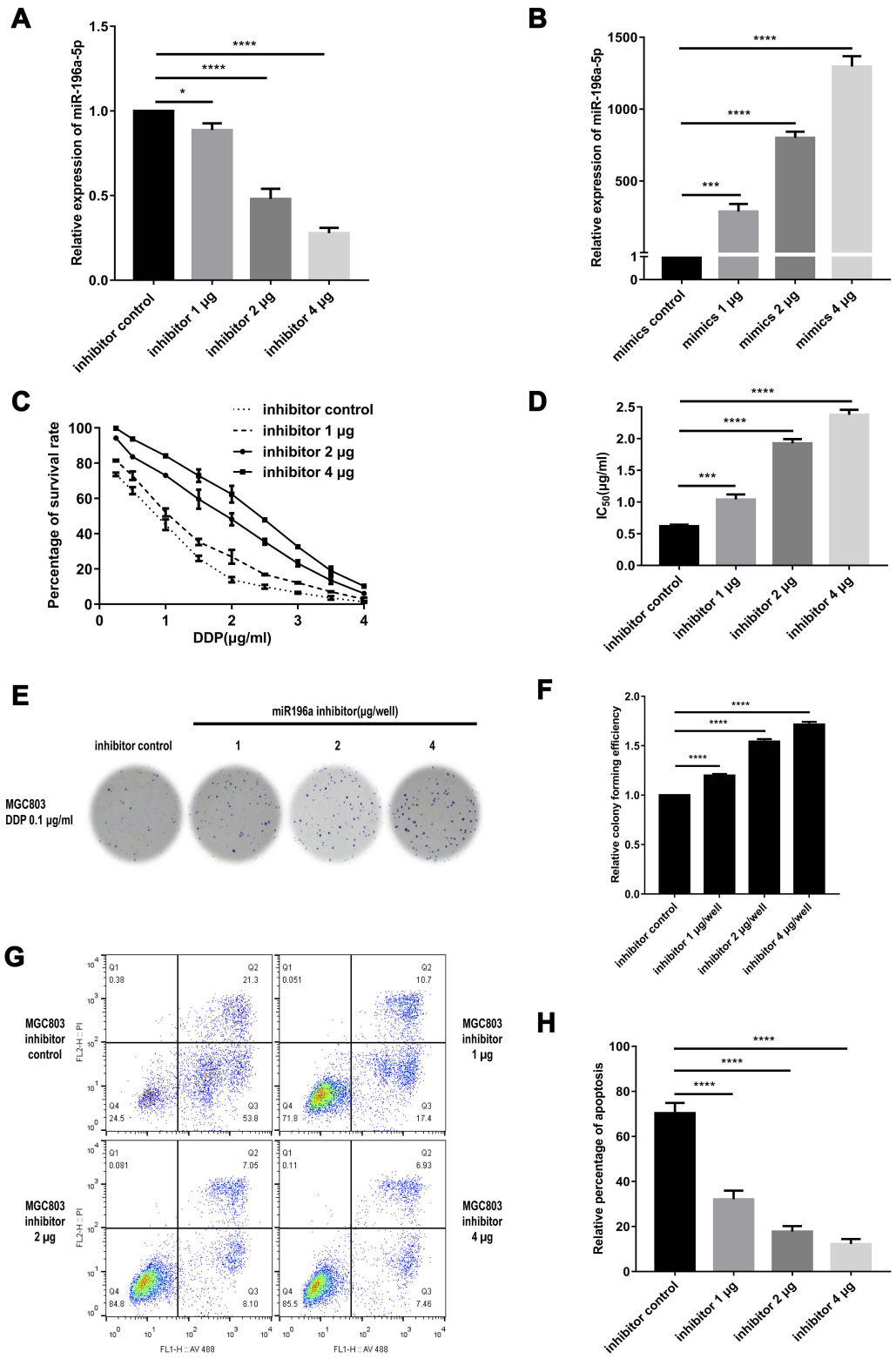

Figure 3 Exogenous downregulation of miR-196a-5p in MGC803 cell line after transient transfection. (**A**) The miR-196a-5p expression following transfected with the three different concentrations of miR-196a-5p inhibitor, as compared with the miR-196a-5p inhibitor control, in MGC803 cells was analyzed by RT-qPCR. (**B**) The relative miR-196a-5p expression after transfected with miR-196a-5p mimic of three different concentrations, compared to the miR-196a-5p mimic control, in MGC803/DDP cell line was analyzed by RT-qPCR. (**C** and **D**) MTT assay was utilized to examine cell activity (**C**) and these IC_{50} values (**D**) of MGC803 cells following transfection with the three different concentrations of miR-196a-5p inhibitor, as compared to the miR-196a-5p inhibitor control. (**E** and **F**) Colony formation assay was carried out for the assessment of the DDP resistance (**E**) and cell activity (**F**) in the MGC803 cells following transfection with the three different concentrations of miR-196a-5p inhibitor, as compared to the miR-196a-5p inhibitor control. (**G** and **H**) Flow cytometry assay was utilized to assess the DDP resistance (**G**) and the cell apoptosis rates (**H**) in MGC803 cell line following transfection with three different concentrations of miR-196a-5p inhibitor, compared to the miR-196a-5p inhibitor control. Each assay was conducted in triplicate. ****P < 0.0001, ***P < 0.001, *P < 0.05 and mean±SD were utilized to show the data.

a bioinformatics screen was performed to identify the downstream target gene of miR-196a-5p. Using TargetScan, HOXB7 was predicted to bind miR-196a-5p at a conserved putative site within the 3′-UTR (Figure 5A).

Furthermore, a dual-luciferase reporter assay was used to determine whether HOXB7 mRNA possessed a functional binding site for miR-196a-5p. The luciferase activity of MGC803 cells co-transfected with HOXB7-WT and the miR-196a-5p mimic was markedly reduced compared with that of GC cells transfected with the NC vector. Co-transfection with HOXB7-MUT and the miR-196a-5p mimic did not reduce luciferase activity significantly. Moreover, the luciferase activity of the WT-group (HOXB7-WT + miR-196a-5p mimic) was markedly lower than that of the MUT-group (HOXB7-MUT + miR-196a-5p mimic) (Figure 5B). These findings indicate that miR-196a-5p indirectly regulates HOXB7.

Western blot and RT-qPCR analysis revealed that miR-196a-5p expression was greater in MGC803 cells than in MGC803/DDP cells, while HOXB7 expression was relatively high in MGC803/DDP cells (Figure 5C). Western blotting revealed that HOXB7 was markedly upregulated in MGC803/DDP compared with MGC803 cells (Figure 5D and E). Moreover, increased levels of HOXB7 protein and mRNA were observed in MGC803 cells transfected with the miR-196a-5p inhibitor (Figure 5F–H), yet were decreased in MGC803/DDP cells following transfection with the miR-196a-5p mimic (Figure 5I–K).

In addition, employing the Kaplan–Meier Plotter confirmed that patients with high miR-196a-5p levels (n=107) exhibited longer OS times over a 10-year period than those with low miR-196a-5p levels. Kaplan–Meier analysis also revealed that low HOXB7 expression levels were associated with improved prognosis in patients with GC (Figure 5L). In summary, these findings strongly suggest that miR-196a-5p levels are inversely associated with HOXB7 expression, and support the conclusion that HOXB7 is a target gene of miR-196a-5p.

miR-196a-5p Modulates DDP Resistance via the miR196a-HOXB7-HER2 Pathway

In a previous study, tumor cells with high HER2 expression were shown to have higher RAS-MAPK and PI3K-AKT signal transduction activities; reduced differentiation, maturation and apoptosis; and increased proliferation and malignant potential. In patients with breast cancer, the miR196a-HOXB7-HER2 axis is also associated with drug resistance.[9] Consistent with these findings, the present study demonstrated that the protein and mRNA expression levels of HER2 were lower in MGC803 cells than in MGC803/DDP cells (Figure 6A–C). Previous studies have shown that in esophageal squamous cell carcinoma, reducing the expression level of apoptotic inhibitor protein Bcl-2 reverses MDR during the treatment process.[45] In addition, miR-634 heightened the response of ovarian cancer DDP-resistant cells by negatively regulating cell-cycle genes (CCND1).[46] Therefore, in the present study, Western blot and RT-qPCR analyses were used to determine the expression levels of CCND1 and Bcl-2. The protein and mRNA levels of CCND1 and Bcl-2 were confirmed to be higher in MGC803/DDP cells than in MGC803 cells (Figure 6E–G and I–K).

To determine whether the activation of the miR196a-HOXB7-HER2 pathway could predict DDP resistance and survival outcome in GC, HER2 expressions level in DDP-treated patients (n=876) were detected using the Kaplan–Meier Plotter. A significant correlation between poor OS and high HER2 expression was observed (HR=1.41, log-rank P=0.00011; Figure 6D); high expression levels of Bcl-2 and CCND1 were also found to be prognostic indicators of poor OS (Figure 6H and L). Collectively, these results verify that the miR196a-HOXB7-HER2 axis serves a vital role in the progression and development of GC chemotherapeutic resistance.

Psoralen Reverses DDP Resistance in GC Cells

DDP can induce apoptosis in tumor cells by depleting their antioxidant capacity; thus, it was speculated that psoralen may enhance DDP-induced apoptosis and reduce drug resistance. To test this hypothesis, MGC803 and MGC803/DDP cells were treated with various concentrations of psoralen (20, 10 and 5 μg/mL) for 4 weeks. MTT assays revealed that psoralen inhibited the proliferation of MGC803 (Figure 7A and B) and MGC803/DDP cells (Figure 8A and B) after 48 h of DDP treatment. Psoralen also reduced the colony forming capacity of MGC803 (Figure 7C and D) and MGC803/DDP cells (Figure 8C and D) after DDP treatment for 48 h. Additionally, flow cytometric analysis demonstrated the apoptotic rate of the MGC803 (Figure 7E and F) and MGC803/DDP cells (Figure 8E and F) was significantly higher in the presence of psoralen than without it. These results indicate that psoralen treatment decreases

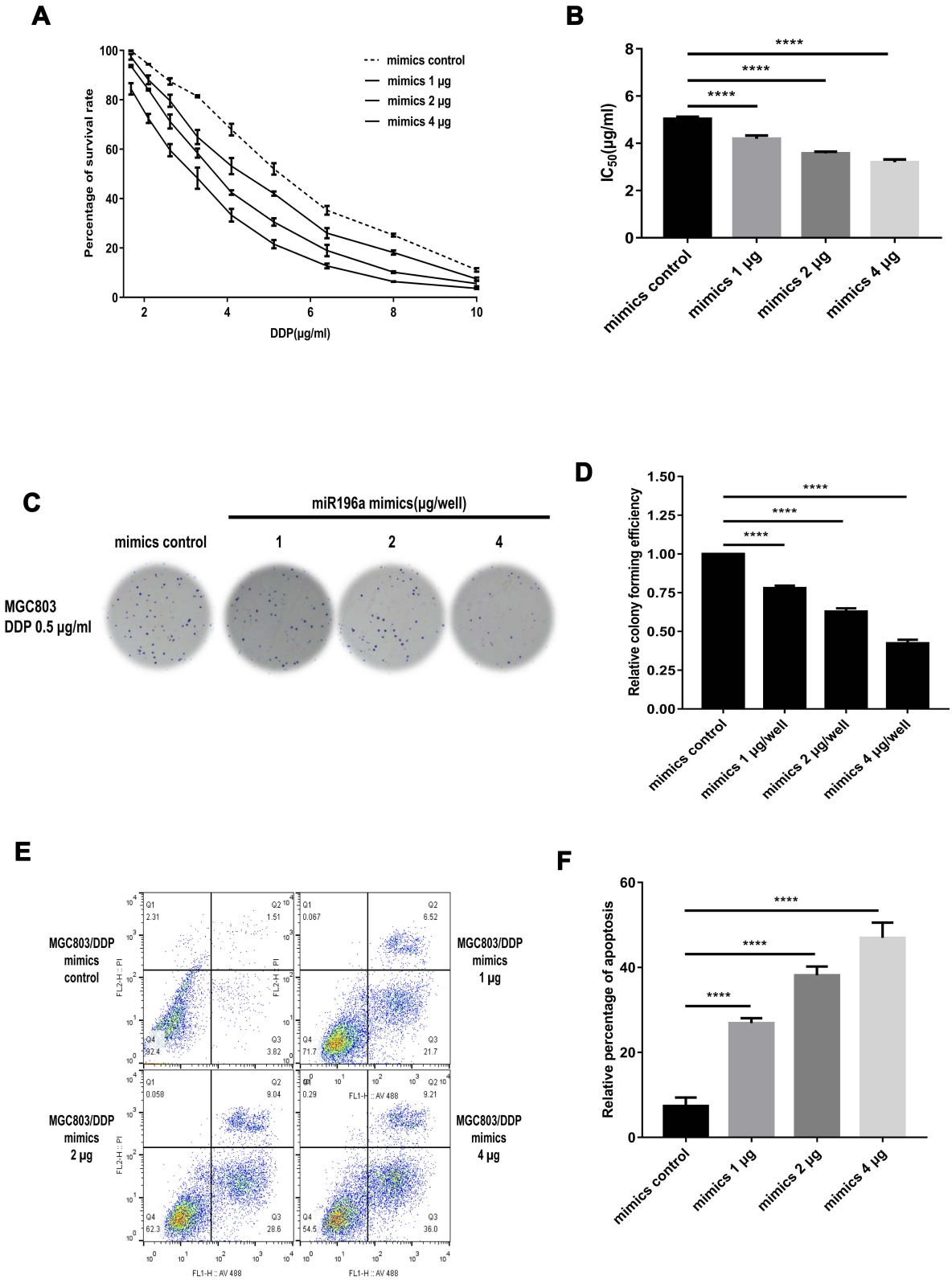

Figure 4 Exogenous overexpression of miR-196a-5p in MGC803/DDP cell line after transient transfection. (**A** and **B**) The cell activity (**A**) and the IC_{50} values (**B**) of MGC803/DDP cells after transfected with miR-196a-5p mimic of three different concentrations and the miR-196a-5p mimic control were calculated via MTT assay. (**C** and **D**) DDP resistance (**C**) and cell proliferation ability (**D**) in MGC803/DDP cell line following transfected with the three different concentrations of miR-196a-5p mimic, compared to the miR-196a-5p mimic control, was evaluated by colony formation assay. (**E** and **F**) Flow cytometry assay was utilized to assess the DDP resistance (**E**) and the cell apoptosis rates (**F**) in MGC803/DDP cell line following transfection with three different concentrations of miR-196a-5p mimic, compared to the miR-196a-5p mimic control. Each assay was conducted in triplicate. ****$P < 0.0001$ and mean±SD were utilized to show the data.

A

	Predicted consequential pairing of target region (top) and miRNA (bottom)	Site type	Context ++ score	Context++ score percentile	Weighted context++ score	Conserved branch length	P_{CT}
Position 221-228 of HOXB7 3' UTR hsa-miR-196a-5p	5' ...CAACACUGAAAAAAUACUACCUA... 3' GGGUUGUUGUACUUUGAUGGAU	8mer	-0.73	99	-0.73	6.505	0.72

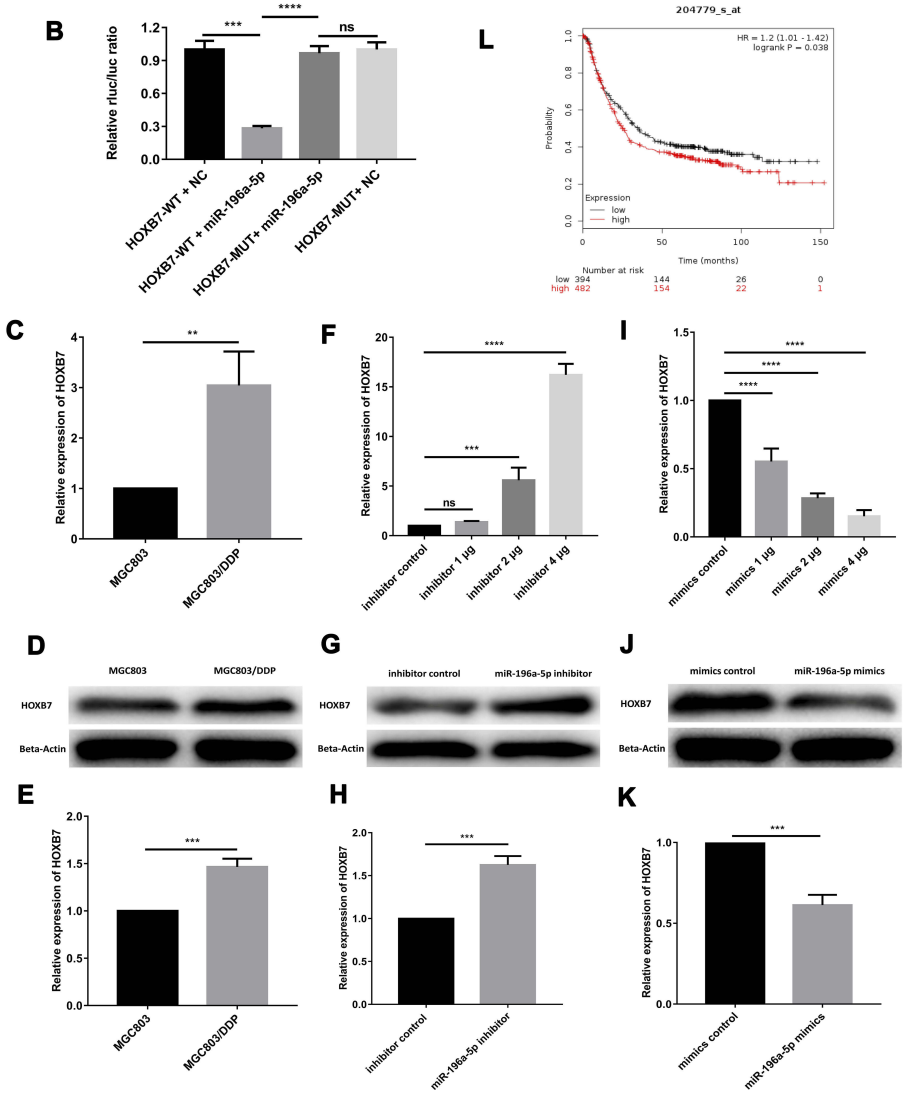

Figure 5 The target gene of miR-196a-5p is HOXB7. (**A**) The predicted results of miR-196a-5p and HOXB7 in TargetScan. (**B**) In dual-luciferase reporter assays, miR-196a-5p suppressed the luciferase activity of the HOXB7-WT vector, and the luciferase activity in the MUT-group (HOXB7-MUT + miR-196a-5p mimic) was greatly higher than that in the WT-group (HOXB7-WT + miR-196a-5p mimic) in MGC803 cell line. (**C**) The relative HOXB7 expression between MGC803 cell line and MGC803/DDP cell line was analyzed by RT-qPCR. (**D** and **E**) The relative expression of HOXB7 between MGC803 cell line and MGC803/DDP cell line was measured by WB. (**F**) The relative expression of HOXB7 following transfection with the three different concentrations of miR-196a-5p inhibitor, compared to the miR-196a-5p inhibitor control, in MGC803 cell line was analyzed by RT-qPCR. (**G** and **H**) The relative expression of HOXB7 in MGC803 cells following transfection with the miR-196a-5p inhibitor and the miR-196a-5p inhibitor control was measured by WB. (**I**) The relative expression of HOXB7 following transfection with the three different concentrations of miR-196a-5p mimic, compared with the miR-196a-5p mimic control, in MGC803/DDP cell line was analyzed by RT-qPCR. (**J** and **K**) WB results of HOXB7 expression levels in MGC803/DDP cell line after transfected with the miR-196a-5p mimic and the miR-196a-5p mimic control. (**L**) Kaplan–Meier survival curves demonstrated lower HOXB7 levels (n=394) were relevant with higher patient survival rates other than higher levels of HOXB7 (n=482) according to Kaplan–Meier Plotter. The beta-actin antibody was utilized for internal reference. Each assay was conducted in triplicate. ****P < 0.0001, ***P < 0.001, **P < 0.01 and mean ±SD were utilized to show the data.

the proliferation and increases apoptosis in CG cells, thus reversing DDP resistance.

Psoralen Reverses DDP Resistance in GC Cell Lines by Activating the miR196a-HOXB7-HER2 Pathway

The miR-196a-5p levels in MGC803 and MGC803/DDP cells were markedly upregulated after 4 weeks of psoralen treatment, when compared to the untreated controls (Figure 9A and B). Therefore, psoralen treatment may be a valid strategy for increasing the expression of miR-196a-5p to reverse DDP resistance in human GC cells. Previous research has shown that photo-activated psoralen can influence the formation of interstrand DNA crosslinks by binding to the HER2 catalytic kinase domain, blocking the HER2 pathway, and thus triggering cancer cell apoptosis. This finding suggests an underlying HER2-targeted mechanism for treating HER2-resistant breast cancers.[47]

In the present study Western blot and RT-qPCR analyses were conducted to determine the impact of psoralen on the expression levels of HER2 signaling pathway-associated genes at the mRNA and protein levels, respectively. Reduced HOXB7, HER2, CCND1 and Bcl-2 mRNA levels were observed in psoralen-cultured MGC803 and MGC803/DDP cells after 48 h of DDP treatment, compared with those in psoralen-uncultured cells (Figure 9C–F). The same trend was observed for HOXB7, HER2, Bcl-2 and CCND1 protein expression (Figure 10A–E). In summary, the expression of HOXB7-HER2 signaling pathway-associated genes at the protein and mRNA levels was significantly affected by 4 weeks of psoralen treatment, suggesting that the psoralen-induced reversal of DDP resistance is associated with the miR196a-HOXB7-HER2 pathway.

Psoralen and DDP Combination Treatment Improves Chemotherapeutic Efficacy and Provides a Clinical Application for Overcoming Chemoresistance in GC Cells

To further understand the association between psoralen and DDP during chemotherapy, the combined effects of psoralen and DDP were investigated in GC cells. The effect of psoralen and DDP was determined by MTT assay and analyzed using CompuSyn software (http://www.combosyn.com), which generates a combination index (CI); the CI is a quantitative indicator of antagonism and synergism in drug combinations, at multiple concentrations at 48 h.[48] After treatment with psoralen, DDP or a combination of both, the CI values of MGC803 (Figure 11A and B) and MGC803/DDP cells (Figure 11C and D) were acquired. A quantitative standard of the extent of drug interaction in light of antagonism (CI>1), additive effect (CI=1) or synergism (CI<1) for a given end-point was obtained.[49] These assays showed that psoralen combined with DDP improves the effect of chemotherapy in both MGC803 and MGC803/DDP cells, compared with psoralen or DDP treatment alone. Since low concentrations of psoralen were less cytotoxic, concentrations of 5 and 10 μg/mL were selected to validate the combined effect of the two drugs. Under treatment with DDP and 10 μg/mL psoralen, the IC_{50} value of DDP was decreased 4.7-fold in MGC803 cells (Figure 11E and F) and 2.2-fold in MGC803/DDP cells (Figure 11G and H), compared with treatment with DDP alone. Notably, MTT results revealed that psoralen increased DDP-induced cytotoxicity and impaired DDP resistance in both MGC803 and MGC803/DDP cells. A colony formation assay confirmed that psoralen combined with DDP decreased proliferation of the two cell lines (Figure 12A–F), compared with psoralen or DDP alone. It was therefore speculated that the combination of psoralen and DDP may enhance DDP-induced apoptosis and decrease drug resistance. Hence, MGC803/DDP and MGC803 cells were treated with psoralen, DDP and the two drugs combined, followed by flow cytometric apoptosis detection. Combination-treatment exerted a synergism effect on apoptotic rate, compared with psoralen or DDP treatment alone (Figure 13A–D). These data indicate that psoralen increases the chemosensitivity of MGC803 cells to DDP, and reverses DDP resistance in MGC803/DDP cells.

Discussion

Development of DDP resistance represents an obstacle for GC treatment. At present, the involvement of non-coding nucleic acids, such as miRNAs, in response to DDP treatment is not well understood. miRNAs serve vital roles in tumor progression and development, and their expression may be associated with chemotherapeutic resistance in tumor cells.[50–53] The survival rates of GC cells were also altered by miR-21 downregulation, which may increase DDP sensitivity.[54] What's more, the PI3K/Akt/survivin pathway was found to be regulated by miR-34a, which influenced DDP-induced GC cell apoptosis.[55] Furthermore, the aberrant expression of miRNAs disrupts

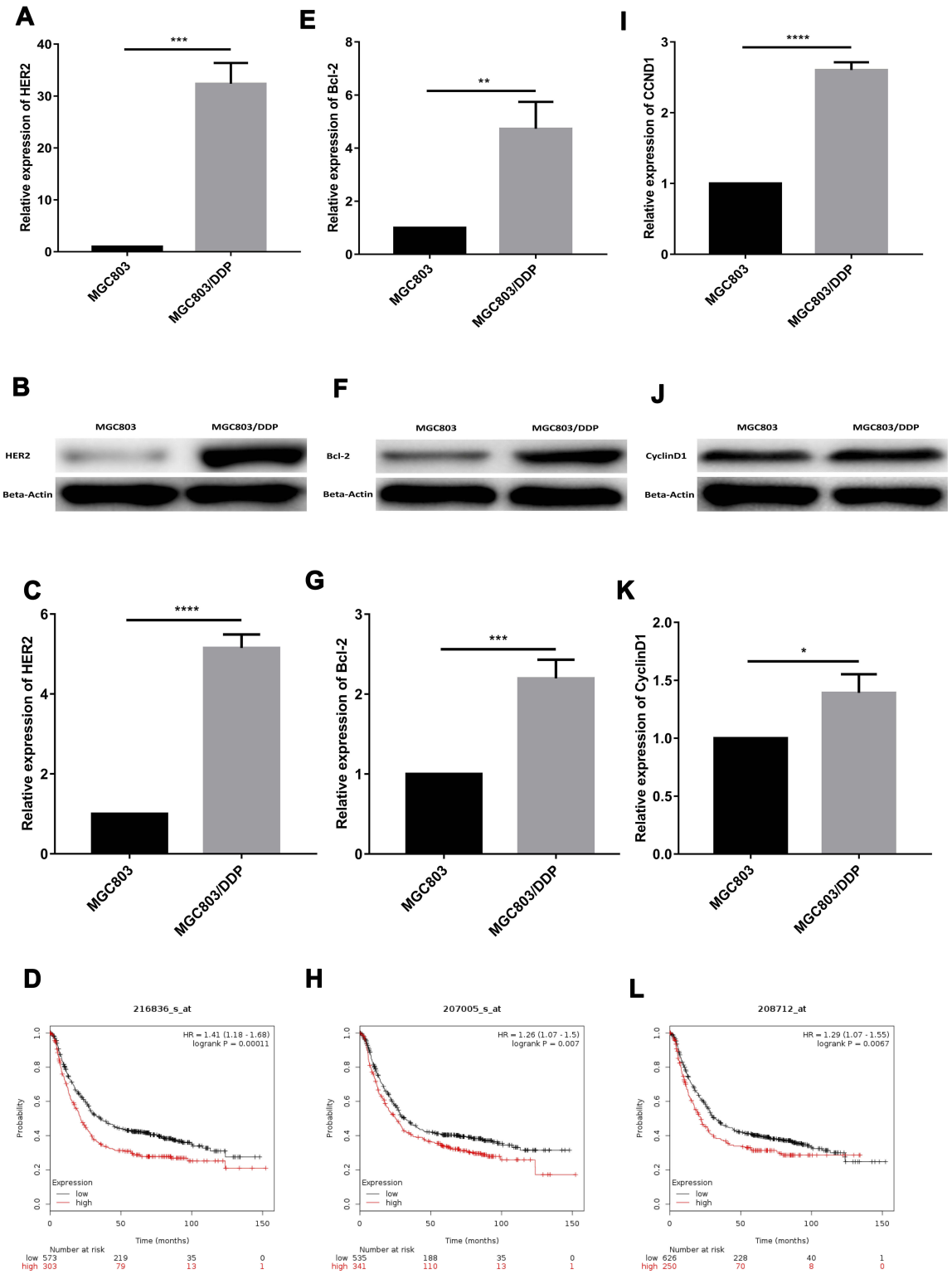

Figure 6 The mechanism of miR-196a-5p changing the cisplatin resistance may be through the miR196a-HOXB7-HER2 signaling pathway. (**A**) The relative expression of HER2 between MGC803 cell line and MGC803/DDP cell line was analyzed by RT-qPCR. (**B** and **C**) Western blot results of HER2 protein levels between MGC803 cell line and MGC803/DDP cell line. (**D**) Kaplan–Meier survival curves showed lower HER2 levels (n=573) were relevant with higher patient survival rates other than higher levels of HER2 (n=303) according to Kaplan–Meier Plotter. (**E**) The relative expression of Bcl-2 between parental MGC803 cells and DDP-resistant MGC803/DDP cells were analyzed by RT-qPCR. (**F** and **G**) Western blot results of Bcl-2 protein levels between MGC803 cell line and MGC803/DDP cell line. (**H**) Kaplan–Meier survival curves suggested lower Bcl-2 levels (n=535) were correlated with higher patient survival rates other than higher Bcl-2 levels (n=341) according to Kaplan–Meier Plotter. (**I**) The relative expression of CCND1 between MGC803 cells and MGC803/DDP cells was analyzed by RT-qPCR. (**J** and **K**) Western blot results of CyclinD1 protein levels between MGC803 cells and MGC803/DDP cells. (**L**) Kaplan–Meier survival curves demonstrated lower levels of CCND1 (n=626) were correlated with higher patient survival rates other than higher levels of CCND1 (n=250) according to Kaplan–Meier Plotter. The beta-actin antibody was utilized for internal reference. Each assay was conducted in triplicate. ****P < 0.0001, ***P < 0.001, **P < 0.01, *P < 0.05 and mean±SD were utilized to show the data.

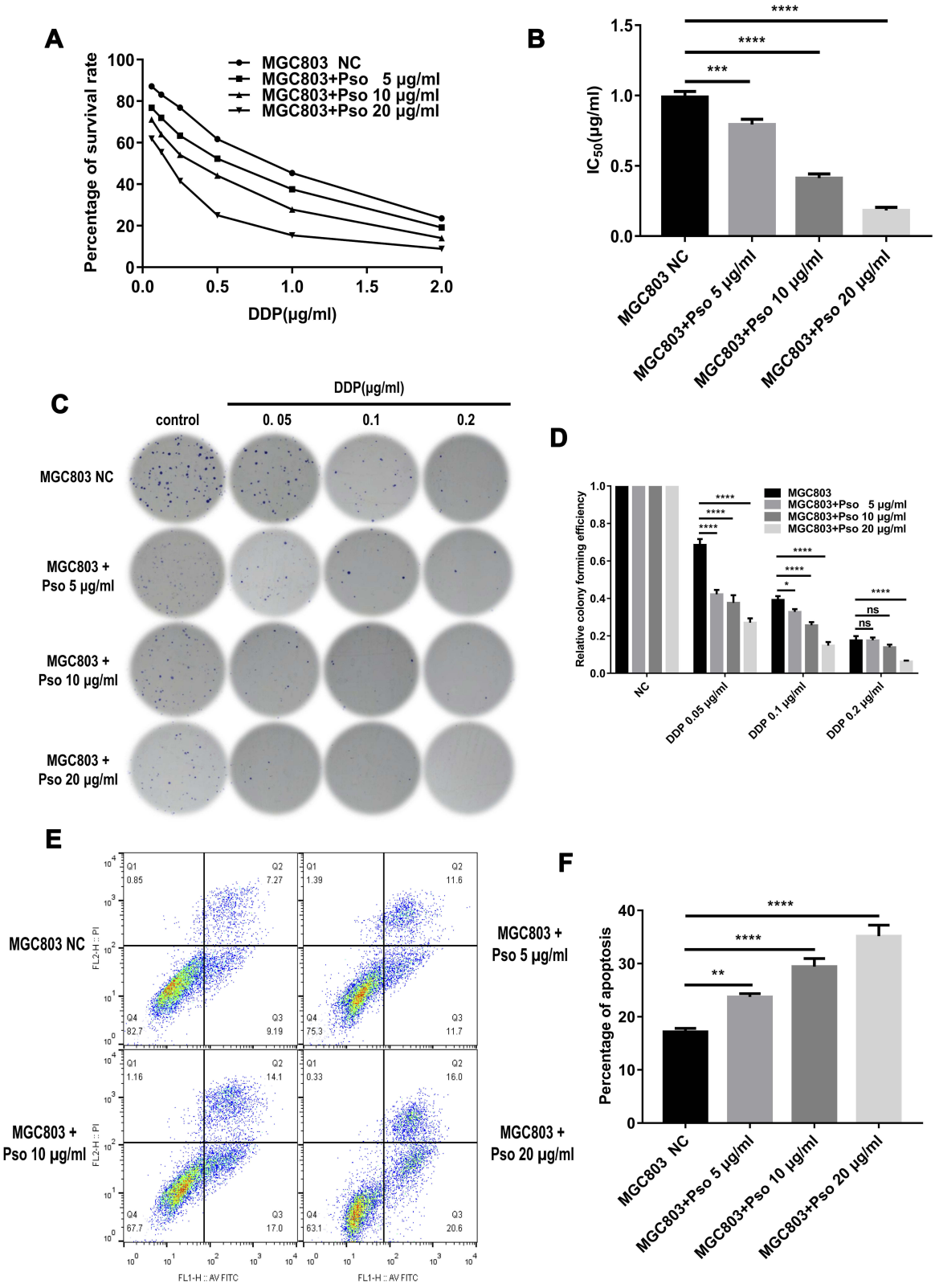

Figure 7 Cultured with psoralen can change the cisplatin resistance of the MGC803 cells. (**A** and **B**) MTT assay was utilized to analyze cell activity (**A**) and the IC_{50} values (**B**) to evaluate anti-proliferative effects of psoralen in MGC803 cells following cultured with psoralen of three different concentrations and the negative control. (**C** and **D**) Colony formation assay was carried out to detect DDP resistance (**C**) and cell proliferation (**D**) in MGC803 cell line following cultured with the three different concentrations of psoralen and the negative control. (**E** and **F**) Flow cytometry assay was utilized to assess the DDP resistance (**E**) and the cell apoptosis rates (**F**) in the MGC803 cells following cultured with the three different concentrations of psoralen and the negative control. Each assay was conducted in triplicate. ****P < 0.0001, ***P < 0.001, **P < 0.01, *P < 0.05 and mean±SD were utilized to show the data.

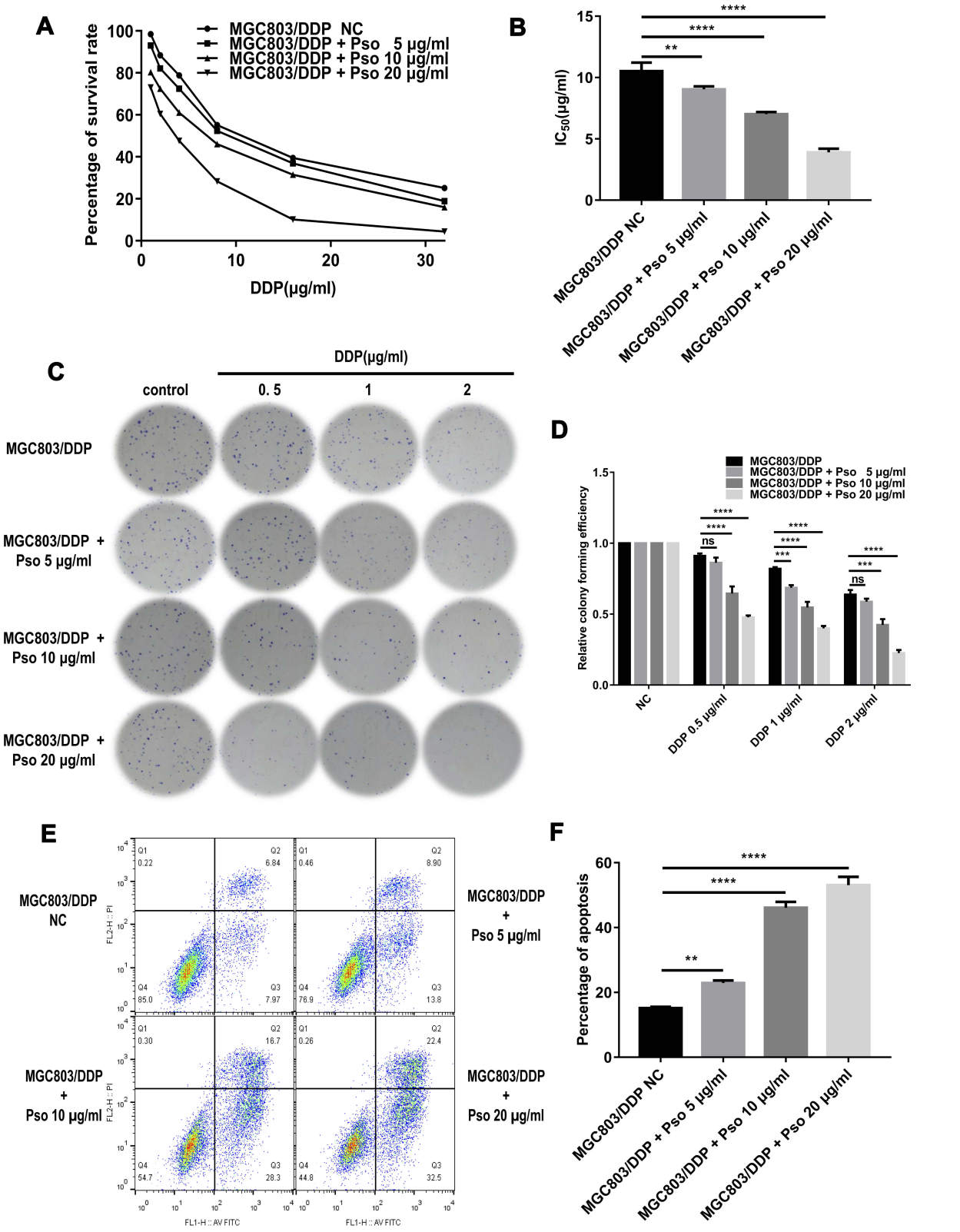

Figure 8 Cultured with psoralen can change the cisplatin resistance of the MGC803/DDP cells. (**A** and **B**) MTT assay was carried out to check cell activity (**A**) and the IC_{50} values (**B**) to evaluate these anti-proliferative effects of psoralen in MGC803/DDP cells following cultured with psoralen of three different concentrations and the negative control. (**C** and **D**) Colony formation assay was utilized to evaluate the DDP resistance (**C**) and the cell proliferation ability (**D**) in the MGC803/DDP cells following cultured with the three different concentrations of psoralen and the negative control. (**E** and **F**) Flow cytometry assay was utilized to assess the DDP resistance (**E**) and the cell apoptosis rates (**F**) in the MGC803/DDP cells following cultured with the three different concentrations of psoralen and the negative control. Each assay was conducted in triplicate. ****P < 0.0001, ***P < 0.001, **P < 0.01 and mean±SD were utilized to show the data.

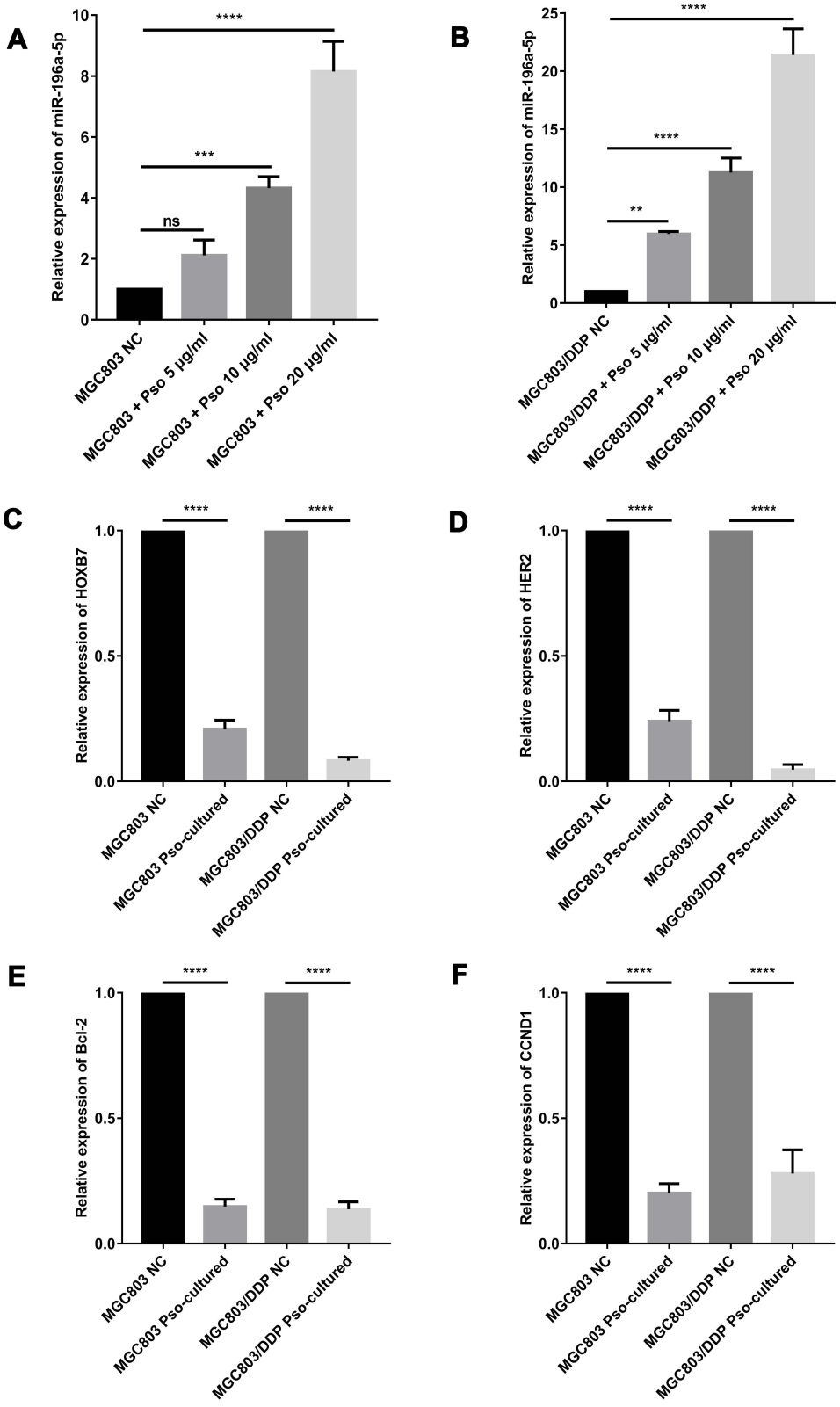

Figure 9 Psoralen could reverse cisplatin resistance of GC cells via activating the miR196a-HOXB7-HER2 Pathway. (**A** and **B**) Using RT-qPCR, the miR-196a-5p relative expression levels after cultured with the three various concentrations of psoralen, compared to the negative control, in MGC803 cell line (**A**) and MGC803/DDP cell line (**B**) were analyzed. (**C–F**) The relative expression of HOXB7 (**C**), HER2 (**D**), Bcl-2 (**E**) and CCND1 (**F**) in MGC803 cell line and MGC803/DDP cell line following cultured with psoralen, as compared with the negative control, was analyzed by RT-qPCR. Each assay was conducted in triplicate. ****P < 0.0001, ***P < 0.001, **P < 0.01 and mean ±SD were utilized to show the data.

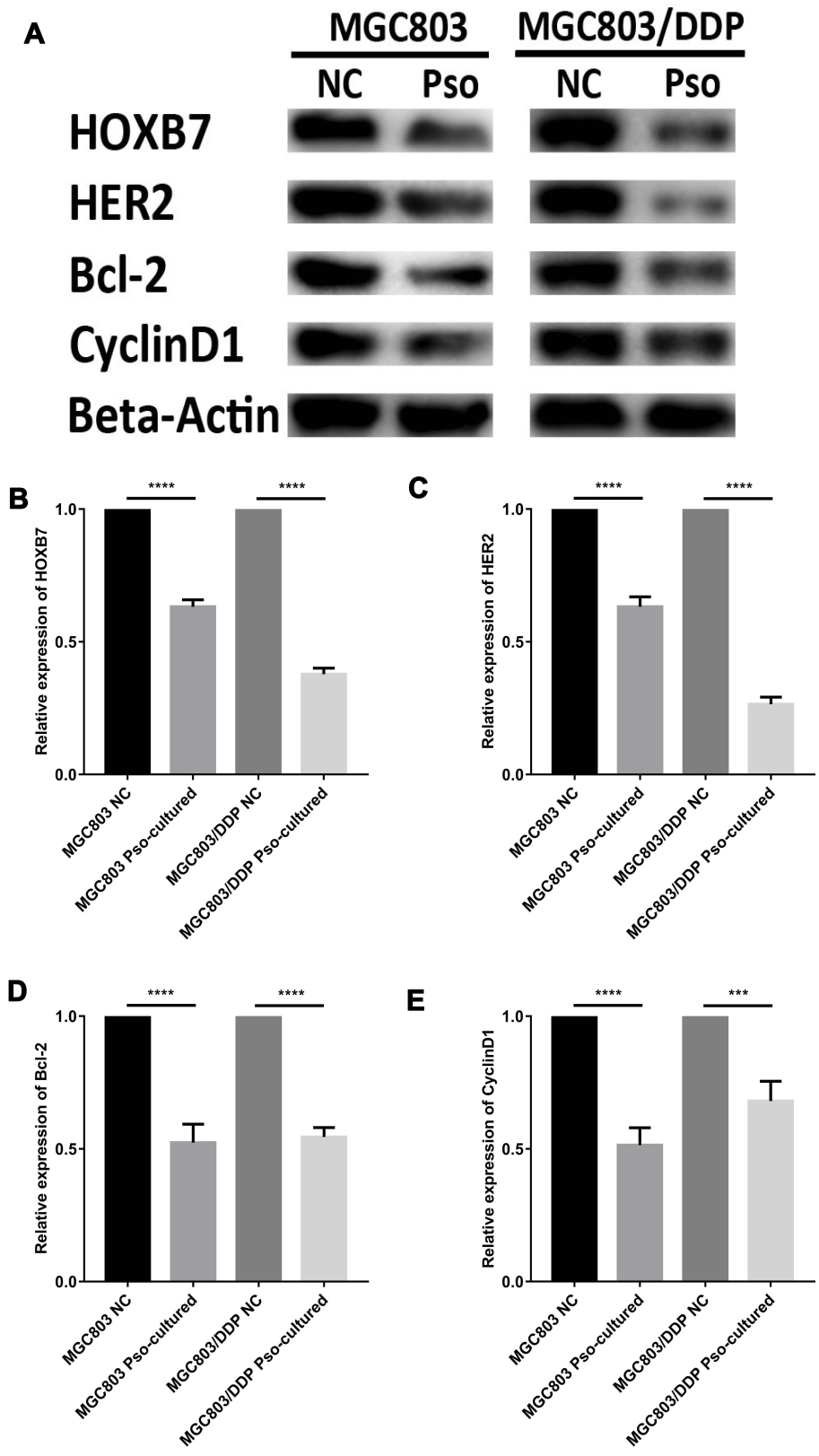

Figure 10 Psoralen could reverse cisplatin resistance of GC cells via activating the miR196a-HOXB7-HER2 Pathway. (**A**) Western blot results of HOXB7, HER2, Bcl-2 and CyclinD1 protein levels between MGC803 cells and MGC803/DDP cells following cultured with psoralen and the negative control. (**B–E**) The relative expression of HOXB7 (**B**), HER2 (**C**), Bcl-2 (**D**) and CyclinD1 (**E**) protein between MGC803 cells and MGC803/DDP cells following cultured with psoralen and the negative control was measured by WB. The beta-actin antibody was utilized for internal reference. Each assay was conducted in triplicate. ****P < 0.0001, ***P < 0.001 and mean±SD were utilized to show the data.

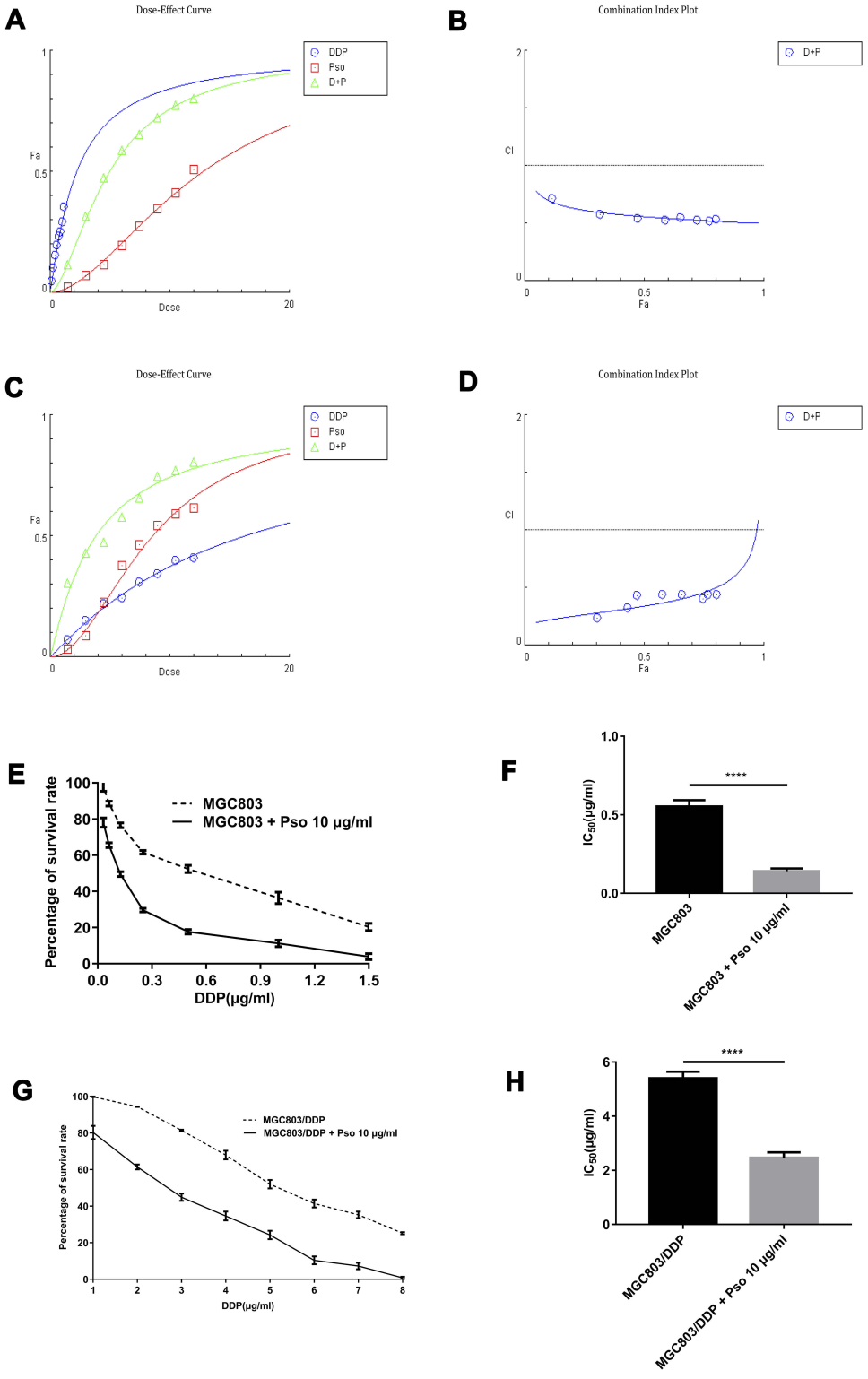

Figure 11 Psoralen combined with DDP improves the effect of chemotherapy and provides a clinical application for gastric cancer resistance to chemotherapy. (**A**) Cell activity was detected via MTT assay by dose-effect curve to investigate the ability of psoralen combined with DDP to affect the chemotherapy in MGC803 cells using the CompuSyn software. (**B**) Using MTT assay, the combination index plots of MGC803 cells following psoralen combined with DDP were calculated. (**C**) Cell activity was examined via MTT assay by dose-effect curve to investigate the ability of psoralen combined with DDP to affect the chemotherapy in MGC803/DDP cells using the CompuSyn software. (**D**) Using MTT assay, the combination index plots of MGC803/DDP cells following psoralen combined with DDP were calculated. (**E** and **F**) Cell activity (**E**) and the IC_{50} values (**F**) were examined to evaluate the combined effects of DDP and 10μg/mL psoralen via MTT assay in MGC803 cells. (**G** and **H**) The cell viability (**G**) and the IC_{50} values (**H**) of MGC803/DDP cell line following DDP alone and DDP combined with 10μg/mL psoralen were calculated by MTT assay. Each assay was conducted in triplicate. ****P < 0.0001 and mean±SD were utilized to show the data.

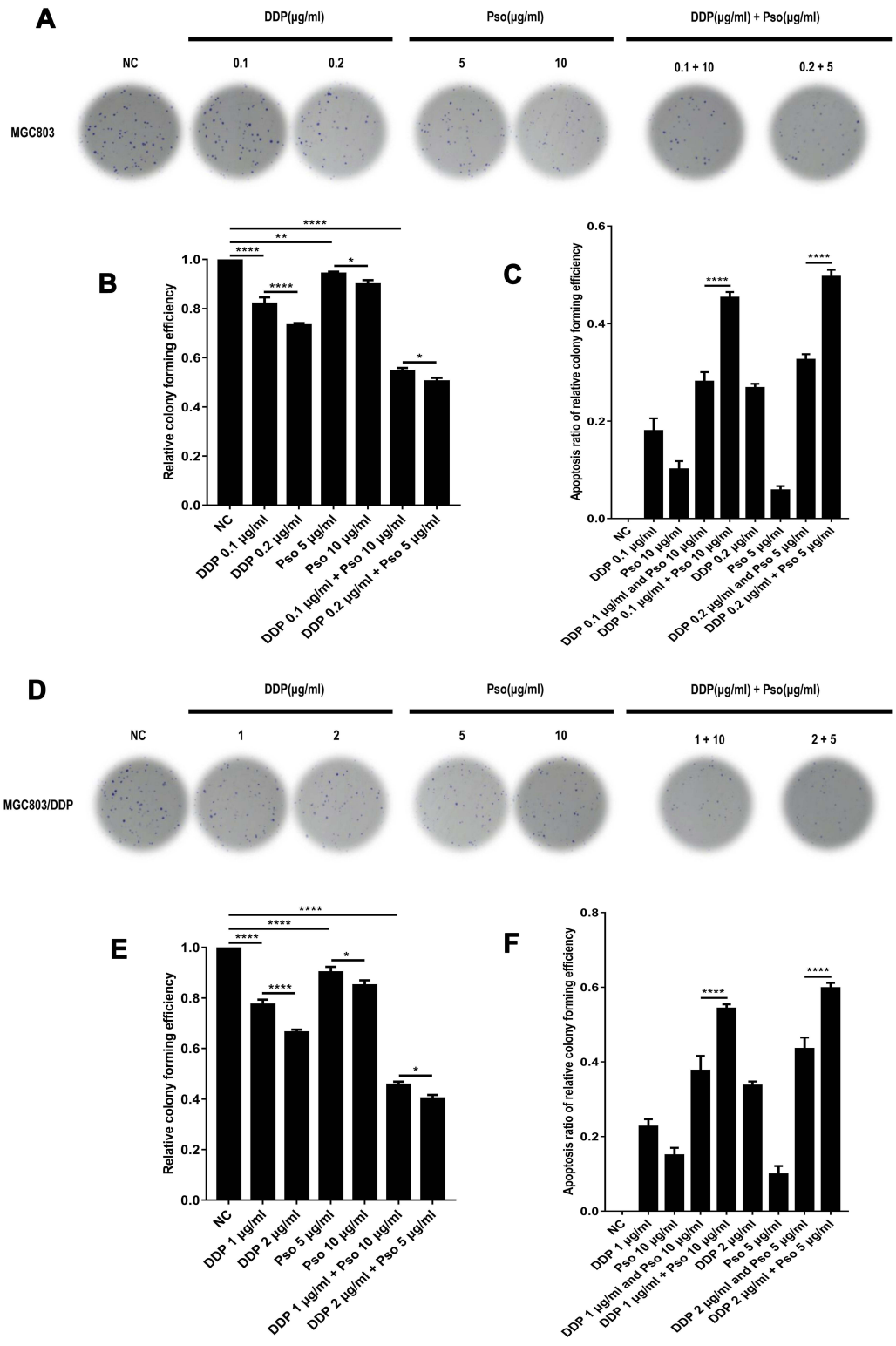

Figure 12 Psoralen combined with DDP improves the effect of chemotherapy and provides a clinical application for gastric cancer resistance to chemotherapy. (**A**) The combination effects of two different concentration of DDP or psoralen alone and DDP combined with psoralen was evaluated by colony formation assay in MGC803 cells. (**B**) Cell proliferation ability using the relative colony forming efficiency was analyzed by colony formation assay in MGC803 cells following two different concentration combination of DDP or psoralen alone and DDP combined with psoralen. (**C**) Cell proliferation ability using the apoptosis ratio of relative colony forming efficiency was inspected by colony formation assay in MGC803 cell-line following two different concentration combination of DDP or psoralen alone and DDP combined with psoralen. (**D**) The combination effects of two different concentration of DDP or psoralen alone and DDP combined with psoralen in MGC803/DDP cells was checked via colony formation assay. (**E**) Cell proliferation ability using the relative colony forming efficiency was inspected by colony formation assay in MGC803/DDP cells following two different concentration combination of DDP or psoralen alone and DDP combined with psoralen. (**F**) Cell proliferation ability using the apoptosis ratio of relative colony forming efficiency was checked by colony formation assay in MGC803/DDP cells following two different concentration combination of DDP or psoralen alone and DDP combined by psoralen. Each assay was conducted in triplicate. ****P < 0.0001, **P < 0.01, *P < 0.05 and mean±SD were utilized to show the data.

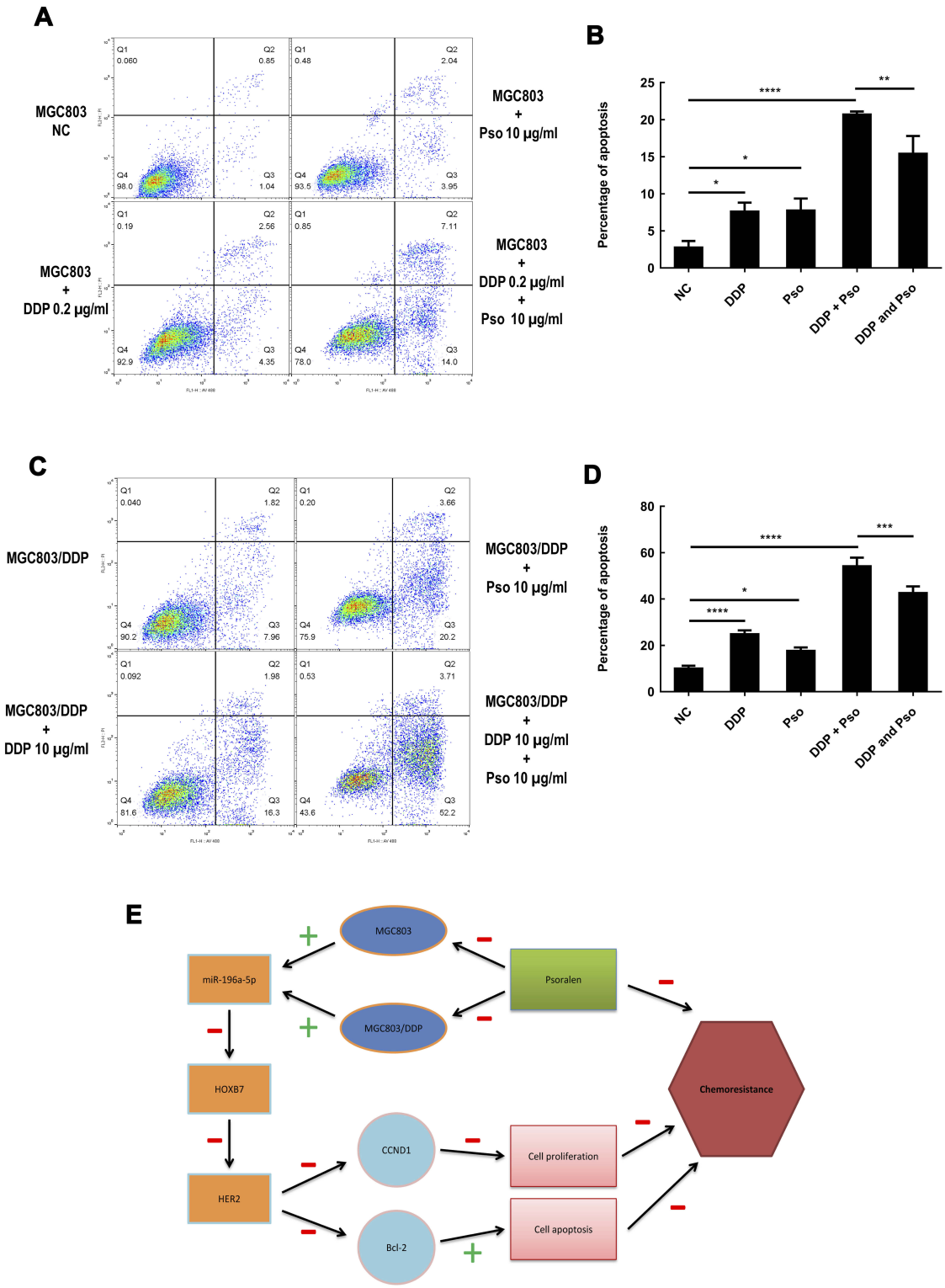

Figure 13 Psoralen combined with DDP improves the effect of chemotherapy and provides a clinical application for gastric cancer resistance to chemotherapy. (**A**) Flow cytometry assay was performed to analyze MGC803 cell line following treated with psoralen (10μg/mL), DDP (0.2μg/mL) and the drug combination to detect the effect of apoptosis. (**B**) Cell apoptosis rates were evaluated using flow cytometry assay in MGC803 cell line following treated with psoralen (10μg/mL), DDP (0.2μg/mL) and the drug combination. (**C**) Flow cytometry assay was utilized to assess the MGC803/DDP cells treated with psoralen (10μg/mL), DDP (10μg/mL) and the drug combination for apoptosis detection. (**D**) Flow cytometry assay was utilized to assess cell apoptosis in the MGC803 cells treated with psoralen (10μg/mL), DDP (10μg/mL) and the drug combination. (**E**) Working model of psoralen functions and schematic of the miR196a-HOXB7-HER2 signaling axis in GC chemoresistance. The green "+" and red "-" represent positive and negative effects, respectively. Each assay was conducted in triplicate. ****P < 0.0001, ***P < 0.001, **P < 0.01, *P < 0.05 and mean±SD were utilized to show the data.

the regulation of RNA networks in various cancer cell types, and thereby contributes to the pathogenesis of human cancer.[56,57]

The present study illustrated that miR-196a-5p expression was reduced in DDP-resistant GC cells and the serum of patients with DDP-resistant GC, and that a low miR-196a-5p level was associated with more malignant clinical parameters and poor prognosis. A recently published review indicated that miR-196a-5p may serve as both a tumor suppressor and an oncomiR.[58] Moreover, the relationship between tumor size and low miR-196a-5p expression in the present study revealed that miR-196a-5p may serve a vital role in tumor cell proliferation. The present study also indicated that miR-196a-5p downregulation increases cell viability and colony forming efficiency, and inhibits apoptosis. Previous studies have found that in breast cancer, the upregulation of miR-196a-5p accelerates tumor growth and metastasis by targeting sprouty-related, EVH1 domain-containing protein 1.[59] In human liver cancer, inhibiting miR-196a-5p reduces cellular invasion and proliferation by targeting forkhead box protein O1.[60] These observations verify that miR-196a-5p exerts an oncogenic effect in various tumors. The results of the present study indicate that miR-196a-5p has an AUC of 0.8552 (Figure 2D), indicating its potential as a non-invasive biomarker for screening and diagnosing GC. Tumor density measurement was a reliable indicator in addition to tumor size alone, as it provided an objective method to quantitatively reflect the tumor response to chemotherapy.[43,61]

In breast cancer cells, abnormal regulation of HOXB7 was shown to influence the incidence of malignances, and epidermal growth factor receptor (EGFR) pathway mediated HOXB7-induced apoptosis. The outcome of cellular transition depends on HOXB7, which hinders tumor development and progression in breast cancer by regulating the HER2 pathway.[10] HOXB7 expression is also regulated by miRNAs; miR-196a-5p mediates the early stages of melanoma progression by targeting HOXB7.[62] In the present study, HOXB7 was predicted as a target gene of miR-196a-5p. Li et al also used TargetScan to predict the downstream targets of miR-196a-5p, and found that these did not include HOXB7.[63] The reason for this discrepancy may be the regular updates to the TargetScan database, which to the best of our knowledge, was last updated in June 2016. In the present study, both HOXB7 mRNA and protein levels were shown to be upregulated in DDP-resistant GC cells. HOXB7 upregulation was significantly associated with shorter survival times in patients with GC. Hence, HOXB7 may be a vital prognostic marker for patients with GC.

The results of the present study indicate a crucial role for HOXB7 in DDP resistance, and that among the upstream regulators of miR-196a-5p, new potential therapeutic targets may be identified. Previous observations indicate that ER target genes are downregulated and upregulated in conjunction with HOXB7 depletion and overexpression, respectively, confirming that HOXB7 serves as an ER cofactor via activation of the ER pathway.[10] The present study identified miR-196a-5p as a potential negative regulator of HOXB7, which binds to the 3′-UTR, leading to downregulated HOXB7 expression.

In the present study, miR-196a-5p overexpression in MGC803/DDP cells reduced the protein expression levels of HER2 and HOXB7. miR-196a-5p downregulation also increased DDP resistance in GC, and the miR196a-HOXB7-HER2 association repressed GC progression by forming a positive feedback loop. Receptor tyrosine-protein kinase erbB-2 is a member of the EGFR family, which was thought to enhance the proliferation rates of tumor cells.[9] Since the upregulation of miR-196a-5p in MGC803/DDP human GC cells reduces the protein and mRNA expression levels of HER2 and HOXB7, it is proposed that miR-196a-5p overexpression may reduce DDP resistance in GC cells via the HOXB7/HER2 pathway, and that miR-196a-5p regulation combined with DDP administration may effectively treat patients with DDP-resistant GC.

Existing literature indicates that natural compounds or herbal medicines may be feasible alternatives to potent chemo-preventive drugs.[64,65] The present study also assessed whether psoralen could reverse DDP resistance via activation of the miR196a-HOXB7-HER2 signaling pathway. Psoralen was found to significantly reduce HER2-mediated DDP resistance in MGC803/DDP cells, and reversed DDP resistance by antagonizing HER2 function. Therefore, psoralen may enhance the efficacy of chemotherapy and minimize HER2-mediated DDP resistance.

The findings of the current study indicate two potential therapeutic regimens for overcoming DDP resistance: Firstly, the use of psoralen to modulate miR-196a-5p expression, and the downregulation of HER2 activity via a HER2 inhibitor. Whether other HER2 inhibitors combined with DDP could exert similar results in DDP-resistant GC is worthy of further study. Secondly, exogenous miR-196a-5p

expression may inhibit HOXB7 expression. Recent research has illustrated that mature miRNA can effectively silence target gene expression.[66] Therefore, a confirmed selective miR-196a-5p response modifier may present a feasible and attractive therapeutic option.

Conclusion

In conclusion, the present study identified miR-196a-5p as an important miRNA involved in the DDP resistance of GC cells. miR-196a-5p shows potential as a serum-based biomarker to predict the therapeutic efficacy of DDP in patients with GC. Furthermore, since overexpression of miR-196a-5p upregulates the sensitivity of DDP-resistant cells, DDP administration combined miR-196a-5p overexpression may be a promising future therapeutic option for patients with DDP-resistant GC. Finally, psoralen can increase chemotherapeutic sensitivity by upregulating miR-196a-5p and then downregulating HOXB7-HER2 signaling axis (Figure 13E). Thus, the use of psoralen to increase chemotherapeutic efficacy, as well as the targeting of the miR196a-HOXB7-HER2 signaling pathway, warrants further investigation for the treatment of DDP-resistant GC.

Acknowledgments

Our work proceeded smoothly with this support from National Natural Science Foundation of China (8160140024) as well as National Key Technologies R&D Program (2015BAI13B09). Our team would like to thank Dr. Xu Bo-Dong for purchasing the DDP-resistant MGC803/DDP cell line. We would also like to acknowledge the assistance of the Biobank Resource and Clinical Data of Beijing Friendship Hospital, Capital Medical University for serum sample collection and data processing.

Author Contributions

All authors contributed to data analysis, drafting or revising the article, gave final approval of the version to be published, and agree to be accountable for all aspects of the work.

Disclosure

The authors report no conflicts of interest in this work.

References

1. Siegel RL, Miller KD, Jemal A. Cancer statistics, 2019. *CA Cancer J Clin*. 2019;69(1):7–34. doi:10.3322/caac.21551
2. Colquhoun A, Arnold M, Ferlay J, Goodman KJ, Forman D, Soerjomataram I. Global patterns of cardia and non-cardia gastric cancer incidence in 2012. *Gut*. 2015;64(12):1881–1888. doi:10.1136/gutjnl-2014-308915
3. Ferlay J, Steliarova-Foucher E, Lortet-Tieulent J, et al. Cancer incidence and mortality patterns in Europe: estimates for 40 countries in 2012. *Eur J Cancer*. 2013;49(6):1374–1403. doi:10.1016/j.ejca.2012.12.027
4. Gunderson LL. Gastric cancer–patterns of relapse after surgical resection. *Semin Radiat Oncol*. 2002;12(2):150–161. doi:10.1053/srao.2002.30817
5. Bang Y-J, Kim Y-W, Yang H-K, et al. Adjuvant capecitabine and oxaliplatin for gastric cancer after D2 gastrectomy (CLASSIC): a Phase 3 open-label, randomised controlled trial. *Lancet*. 2012;379(9813):315–321. doi:10.1016/S0140-6736(11)61873-4
6. Dasari S, Tchounwou PB. Cisplatin in cancer therapy: molecular mechanisms of action. *Eur J Pharmacol*. 2014;740:364–378. doi:10.1016/j.ejphar.2014.07.025
7. Zong L, Abe M, Seto Y, Ji J. The challenge of screening for early gastric cancer in China. *Lancet*. 2016;388(10060):2606. doi:10.1016/S0140-6736(16)32226-7
8. Kovalchuk O, Filkowski J, Meservy J, et al. Involvement of microRNA-451 in resistance of the MCF-7 breast cancer cells to chemotherapeutic drug doxorubicin. *Mol Cancer Ther*. 2008;7(7):2152–2159. doi:10.1158/1535-7163.MCT-08-0021
9. Meng S, Tripathy D, Shete S, et al. HER-2 gene amplification can be acquired as breast cancer progresses. *Proc Natl Acad Sci U S A*. 2004;101(25):9393–9398. doi:10.1073/pnas.0402993101
10. Jin K, Park S, Teo WW, et al. HOXB7 is an ERalpha cofactor in the activation of HER2 and multiple ER target genes leading to endocrine resistance. *Cancer Discov*. 2015;5(9):944–959. doi:10.1158/2159-8290.CD-15-0090
11. He X, Liu Z, Xia Y, et al. HOXB7 overexpression promotes cell proliferation and correlates with poor prognosis in gastric cancer patients by inducing expression of both AKT and MARKs. *Oncotarget*. 2017;8(1):1247–1261. doi:10.18632/oncotarget.13604
12. Bartel DP. MicroRNAs: genomics, biogenesis, mechanism, and function. *Cell*. 2004;116(2):281–297. doi:10.1016/S0092-8674(04)00045-5
13. Muhammad N, Bhattacharya S, Steele R, Ray RB. Anti-miR-203 suppresses ER-positive breast cancer growth and stemness by targeting SOCS3. *Oncotarget*. 2016;7(36):58595–58605. doi:10.18632/oncotarget.11193
14. Krzeszinski JY, Wei W, Huynh H, et al. miR-34a blocks osteoporosis and bone metastasis by inhibiting osteoclastogenesis and Tgif2. *Nature*. 2014;512(7515):431–435. doi:10.1038/nature13375
15. Verma AM, Patel M, Aslam MI, et al. Circulating plasma microRNAs as a screening method for detection of colorectal adenomas. *Lancet*. 2015;385:S100. doi:10.1016/S0140-6736(15)60415-9
16. Zhang L, Zhang S, Yao J, et al. Microenvironment-induced PTEN loss by exosomal microRNA primes brain metastasis outgrowth. *Nature*. 2015;527(7576):100–104. doi:10.1038/nature15376
17. Wu SY, Rupaimoole R, Shen F, et al. A miR-192-EGR1-HOXB9 regulatory network controls the angiogenic switch in cancer. *Nat Commun*. 2016;7(1):11169. doi:10.1038/ncomms11169
18. Pi J, Tao T, Zhuang T, et al. A microRNA302-367-Erk1/2-Klf2-S1pr1 pathway prevents tumor growth via restricting angiogenesis and improving vascular stability. *Circ Res*. 2017;120(1):85–98. doi:10.1161/CIRCRESAHA.116.309757
19. Valeri N, Braconi C, Gasparini P, et al. MicroRNA-135b promotes cancer progression by acting as a downstream effector of oncogenic pathways in colon cancer. *Cancer Cell*. 2014;25(4):469–483. doi:10.1016/j.ccr.2014.03.006
20. Bartolome-Izquierdo N, de Yebenes VG, Alvarez-Prado AF, et al. miR-28 regulates the germinal center reaction and blocks tumor growth in preclinical models of non-Hodgkin lymphoma. *Blood*. 2017;129(17):2408–2419. doi:10.1182/blood-2016-08-731166
21. Au Yeung CL, Co NN, Tsuruga T, et al. Exosomal transfer of stroma-derived miR21 confers paclitaxel resistance in ovarian cancer cells through targeting APAF1. *Nat Commun*. 2016;7:11150. doi:10.1038/ncomms11150

22. Sahu N, Stephan JP, Cruz DD, et al. Functional screening implicates miR-371-3p and peroxiredoxin 6 in reversible tolerance to cancer drugs. *Nat Commun*. 2016;7:12351. doi:10.1038/ncomms12351
23. Sorrentino A, Liu CG, Addario A, Peschle C, Scambia G, Ferlini C. Role of microRNAs in drug-resistant ovarian cancer cells. *Gynecol Oncol*. 2008;111(3):478–486. doi:10.1016/j.ygyno.2008.08.017
24. Yu ZW, Zhong LP, Ji T, Zhang P, Chen WT, Zhang CP. MicroRNAs contribute to the chemoresistance of cisplatin in tongue squamous cell carcinoma lines. *Oral Oncol*. 2010;46(4):317–322. doi:10.1016/j.oraloncology.2010.02.002
25. Giovannetti E, Erozenci A, Smit J, Danesi R, Peters GJ. Molecular mechanisms underlying the role of microRNAs (miRNAs) in anticancer drug resistance and implications for clinical practice. *Crit Rev Oncol Hematol*. 2012;81(2):103–122. doi:10.1016/j.critrevonc.2011.03.010
26. Tanzer A, Amemiya CT, Kim CB, Stadler PF. Evolution of microRNAs located within Hox gene clusters. *J Exp Zool B Mol Dev Evol*. 2005;304B(1):75–85. doi:10.1002/jez.b.21021
27. Sehm T, Sachse C, Frenzel C, Echeverri K. miR-196 is an essential early-stage regulator of tail regeneration, upstream of key spinal cord patterning events. *Dev Biol*. 2009;334(2):468–480. doi:10.1016/j.ydbio.2009.08.008
28. Stiegelbauer V, Vychytilova-Faltejskova P, Karbiener M, et al. miR-196b-5p regulates colorectal cancer cell migration and metastases through interaction with HOXB7 and GALNT5. *Clin Cancer Res*. 2017;23(17):5255–5266. doi:10.1158/1078-0432.CCR-17-0023
29. Li JH, Luo N, Zhong MZ, et al. Inhibition of microRNA-196a might reverse cisplatin resistance of A549/DDP non-small-cell lung cancer cell line. *Tumour Biol*. 2016;37(2):2387–2394. doi:10.1007/s13277-015-4017-7
30. Ueda T, Volinia S, Okumura H, et al. Relation between microRNA expression and progression and prognosis of gastric cancer: a microRNA expression analysis. *Lancet Oncol*. 2010;11(2):136–146. doi:10.1016/S1470-2045(09)70343-2
31. Goswami RS, Atenafu EG, Xuan Y, et al. MicroRNA signature obtained from the comparison of aggressive with indolent non-Hodgkin lymphomas: potential prognostic value in mantle-cell lymphoma. *J clin oncol*. 2013;31(23):2903–2911. doi:10.1200/JCO.2012.45.3050
32. Hur K, Toiyama Y, Schetter AJ, et al. Identification of a metastasis-specific MicroRNA signature in human colorectal cancer. *J Natl Cancer Inst*. 2015;107:3. doi:10.1093/jnci/dju492
33. Toiyama Y, Takahashi M, Hur K, et al. Serum miR-21 as a diagnostic and prognostic biomarker in colorectal cancer. *J Natl Cancer Inst*. 2013;105(12):849–859. doi:10.1093/jnci/djt101
34. Lin X-J, Chong Y, Guo Z-W, et al. A serum microRNA classifier for early detection of hepatocellular carcinoma: a multicentre, retrospective, longitudinal biomarker identification study with a nested case-control study. *Lancet Oncol*. 2015;16(7):804–815. doi:10.1016/S1470-2045(15)00048-0
35. Hu Z, Chen X, Zhao Y, et al. Serum microRNA signatures identified in a genome-wide serum microRNA expression profiling predict survival of non-small-cell lung cancer. *J Clin Oncol*. 2010;28(10):1721–1726. doi:10.1200/JCO.2009.24.9342
36. Chai S, To KK, Lin G. Circumvention of multi-drug resistance of cancer cells by Chinese herbal medicines. *Chin Med*. 2010;5:26. doi:10.1186/1749-8546-5-26
37. Bhattacharya S, Muhammad N, Steele R, Peng G, Ray RB. Immunomodulatory role of bitter melon extract in inhibition of head and neck squamous cell carcinoma growth. *Oncotarget*. 2016;7(22):33202–33209. doi:10.18632/oncotarget.8898
38. Muhammad N, Steele R, Isbell TS, Philips N, Ray RB. Bitter melon extract inhibits breast cancer growth in preclinical model by inducing autophagic cell death. *Oncotarget*. 2017;8(39):66226–66236. doi:10.18632/oncotarget.19887
39. Bhattacharya S, Muhammad N, Steele R, Kornbluth J, Ray RB. Bitter melon enhances natural killer-mediated toxicity against head and neck cancer cells. *Cancer Prev Res (Phila)*. 2017;10(6):337–344. doi:10.1158/1940-6207.CAPR-17-0046
40. McGinnis KS, Shapiro M, Vittorio CC, Rook AH, Junkins-Hopkins JM. Psoralen plus long-wave UV-A (PUVA) and bexarotene therapy: an effective and synergistic combined adjunct to therapy for patients with advanced cutaneous T-cell lymphoma. *Arch Dermatol*. 2003;139(6):771–775. doi:10.1001/archderm.139.6.771
41. Querfeld C, Rosen ST, Kuzel TM, et al. Long-term follow-up of patients with early-stage cutaneous T-cell lymphoma who achieved complete remission with psoralen plus UV-A monotherapy. *Arch Dermatol*. 2005;141(3):305–311. doi:10.1001/archderm.141.3.305
42. Wu JZ, Situ ZQ, Chen JY, Liu B, Wang W. Chemosensitivity of salivary gland and oral cancer cell lines. *Chin Med J*. 1992;105(12):1026–1028.
43. Choi H, Charnsangavej C, SdC F, et al. CT evaluation of the response of gastrointestinal stromal tumors after imatinib mesylate treatment: a quantitative analysis correlated with FDG PET findings. *Am J Roentgenol*. 2004;183(6):1619–1628. doi:10.2214/ajr.183.6.01831619
44. Szafranska-Schwarzbacht AE, Adai AT, Lee LS, Conwell DL, Andruss BF. Development of a miRNA-based diagnostic assay for pancreatic ductal adenocarcinoma. *Expert Rev Mol Diagn*. 2011;11(3):249–257. doi:10.1586/erm.11.10
45. Zhang H, Li M, Han Y, et al. Down-regulation of miR-27a might reverse multidrug resistance of esophageal squamous cell carcinoma. *Dig Dis Sci*. 2010;55(9):2545–2551. doi:10.1007/s10620-009-1051-6
46. van Jaarsveld MT, van Kuijk PF, Boersma AW, et al. miR-634 restores drug sensitivity in resistant ovarian cancer cells by targeting the Ras-MAPK pathway. *Mol Cancer*. 2015;14:196. doi:10.1186/s12943-015-0464-4
47. Xia W, Gooden D, Liu L, et al. Photo-activated psoralen binds the ErbB2 catalytic kinase domain, blocking ErbB2 signaling and triggering tumor cell apoptosis. *PLoS One*. 2014;9(2):e88983. doi:10.1371/journal.pone.0088983
48. Chou TC. Drug combination studies and their synergy quantification using the Chou-Talalay method. *Cancer Res*. 2010;70(2):440–446. doi:10.1158/0008-5472.CAN-09-1947
49. Ashton JC. Drug combination studies and their synergy quantification using the Chou-Talalay method–letter. *Cancer Res*. 2015;75(11):2400. doi:10.1158/0008-5472.CAN-14-3763
50. Jay C, Nemunaitis J, Chen P, Fulgham P, Tong AW. miRNA profiling for diagnosis and prognosis of human cancer. *DNA Cell Biol*. 2007;26(5):293–300. doi:10.1089/dna.2006.0554
51. Xia L, Zhang D, Du R, et al. miR-15b and miR-16 modulate multidrug resistance by targeting BCL2 in human gastric cancer cells. *Int J Cancer*. 2008;123(2):372–379. doi:10.1002/ijc.23501
52. Yang H, Kong W, He L, et al. MicroRNA expression profiling in human ovarian cancer: miR-214 induces cell survival and cisplatin resistance by targeting PTEN. *Cancer Res*. 2008;68(2):425–433. doi:10.1158/0008-5472.CAN-07-2488
53. Li T, Li D, Sha J, Sun P, Huang Y. MicroRNA-21 directly targets MARCKS and promotes apoptosis resistance and invasion in prostate cancer cells. *Biochem Biophys Res Commun*. 2009;383(3):280–285. doi:10.1016/j.bbrc.2009.03.077
54. Yang SM, Huang C, Li XF, Yu MZ, He Y, Li J. miR-21 confers cisplatin resistance in gastric cancer cells by regulating PTEN. *Toxicology*. 2013;306:162–168. doi:10.1016/j.tox.2013.02.014
55. Cao W, Yang W, Fan R, et al. miR-34a regulates cisplatin-induce gastric cancer cell death by modulating PI3K/AKT/survivin pathway. *Tumour Biol*. 2014;35(2):1287–1295. doi:10.1007/s13277-013-1171-7
56. Esquela-Kerscher A, Slack FJ. Oncomirs - microRNAs with a role in cancer. *Nat Rev Cancer*. 2006;6(4):259–269. doi:10.1038/nrc1840
57. Hu X, Miao J, Zhang M, et al. miRNA-103a-3p promotes human gastric cancer cell proliferation by targeting and suppressing ATF7 in vitro. *Mol Cells*. 2018;41(5):390–400. doi:10.14348/molcells.2018.2078

58. Svoronos AA, Engelman DM, Slack FJ. OncomiR or tumor suppressor? The duplicity of MicroRNAs in cancer. *Cancer Res*. 2016;76 (13):3666–3670. doi:10.1158/0008-5472.CAN-16-0359
59. Jiang CF, Shi ZM, Li DM, et al. Estrogen-induced miR-196a elevation promotes tumor growth and metastasis via targeting SPRED1 in breast cancer. *Mol Cancer*. 2018;17(1):83. doi:10.1186/s12943-018-0830-0
60. Yang L, Peng F, Qin J, Zhou H, Wang B. Downregulation of microRNA-196a inhibits human liver cancer cell proliferation and invasion by targeting FOXO1. *Oncol Rep*. 2017;38(4):2148–2154. doi:10.3892/or.2017.5873
61. Schwartz LH, Litiere S, de Vries E, et al. RECIST 1.1—Update and clarification: from the RECIST committee. *Eur J Cancer*. 2016; 62:132–137. doi:10.1016/j.ejca.2016.03.081
62. Braig S, Mueller DW, Rothhammer T, Bosserhoff A-K. MicroRNA miR-196a is a central regulator of HOX-B7 and BMP4 expression in malignant melanoma. *Cell Mol Life Sci*. 2010;67(20):3535–3548. doi:10.1007/s00018-010-0394-7
63. Li H-L, Xie S-P, Yang Y-L, et al. Clinical significance of upregulation of mir-196a-5p in gastric cancer and enriched KEGG pathway analysis of target genes. *Asian Pac J Cancer Prev*. 2015;16 (5):1781–1787. doi:10.7314/APJCP.2015.16.5.1781
64. Montazeri AS, Raei M, Ghanbari A, Dadgari A, Montazeri AS, Hamidzadeh A. Effect of herbal therapy to intensity chemotherapy-induced nausea and vomiting in cancer patients. *Iran Red Crescent Med J*. 2013;15(2):101–106. doi:10.5812/ircmj.4392
65. Chen WT, Yang TS, Chen HC, et al. Effectiveness of a novel herbal agent MB-6 as a potential adjunct to 5-fluoracil-based chemotherapy in colorectal cancer. *Nutr Res*. 2014;34(7):585–594. doi:10.1016/j.nutres.2014.06.010
66. Hashemi ZS, Moghadam MF, Farokhimanesh S, Rajabibazl M, Sadroddiny E. Inhibition of breast cancer metastasis by co-transfection of miR-31/193b-mimics. *Iran J Basic Med Sci*. 2018;21(4):427–433. doi:10.22038/IJBMS.2018.26614.6522